



Supplementary Materials for

Anticancer immunotherapy by CTLA-4 blockade relies on the gut microbiota

Marie Vétizou, Jonathan M. Pitt, Romain Daillère, Patricia Lepage, Nadine Waldschmitt, Caroline Flament, Sylvie Rusakiewicz, Bertrand Routy, Maria P. Roberti, Connie P. M. Duong, Vichnou Poirier-Colame, Antoine Roux, Sonia Becharef, Silvia Formenti, Encouse Golden, Sascha Cording, Gerard Eberl, Andreas Schlitzer, Florent Ginhoux, Sridhar Mani, Takahiro Yamazaki, Nicolas Jacquelot, David P. Enot, Marion Bérard, Jérôme Nigou, Paule Opolon, Alexander Eggermont, Paul-Louis Woerther, Elisabeth Chachaty, Nathalie Chaput, Caroline Robert, Christina Mateus, Guido Kroemer, Didier Raoult, Ivo Gomperts Boneca, Franck Carbonnel, Mathias Chamaillard, Laurence Zitvogel*

*Corresponding author. E-mail: laurence.zitvogel@gustaveroussy.fr

Published 5 November 2015 on *Science Express*

DOI: 10.1126/science.aad1329

This PDF file includes

Materials and Methods

Figs. S1 to S22

Tables S1 to S5

References

Supplemental materials Vétizou et al.

One Sentence Summary: *Bacteroides* involved in anti-CTLA4 Ab-mediated cancer immunosurveillance.

Abbreviations list: ACS: antibiotic treatment with ampicillin, colistin and streptomycin, Bc: *Burkholderia cepacia*, Bf: *Bacteroides fragilis*, BM-DC: Bone marrow-derived dendritic cells, CTLA4: Cytotoxic T-Lymphocyte Antigen-4, DC: Dendritic cells, EMA: European Medicine Agency, FDA: Food and drug administration, FITC: fluorescein isothiocyanate, FMT: fecal microbial transplantation, GF: Germ-free, GM-CSF: Granulocyte-macrophage colony-stimulating factor, HV: Healthy volunteers, IBD: Inflammatory bowel diseases, ICB: Immune checkpoint blocker, ICOS: Inducible T-cell costimulatory, IEC: intestinal epithelial cells, IEL: intraepithelial lymphocytes, IL-12: Interleukin-12, LP: Lamina propria, mAb: Monoclonal antibody, MHC II: class II molecules, mLN: Mesenteric lymph node, MM: Metastatic melanoma, MOI: Multiplicity of infection, NOD2: Nucleotide-binding oligomerization domain-containing protein 2, PCA: Principle component analysis, PD1: Programmed cell death protein 1, PS: Polysaccharide, PBMC: peripheral blood mononuclear cells, SPF: Specific pathogen free, Tc1: Type 1 cytotoxic T-cells, Th1: T helper type 1, TLR: Toll like receptor, Tr1: Type 1 regulatory T-cells, Tregs: Regulatory T cells, WT: Wild type.

Key words: CTLA4, ipilimumab, cancer, immunity, *Bacteroides fragilis*, *Bacteroides thetaiotaomicron*, *Burkholderia cepacia*, microbiome, IL-12.

Acknowledgments: We are grateful to the staff of the animal facility of Gustave Roussy and Institut Pasteur. We thank P. Gonin, B. Ryffel, T. Angelique, N. Chanthapathet, H. Li and S. Zuberogitia for technical help. The data presented in this manuscript are tabulated in the main paper and in the supplementary materials. DNA sequence reads from this study have been submitted to the NCBI under the Bioproject ID PRJNA299112. LZ, MV and PL have filed patent applications n° EP 14190167 that relates to specific topic: Methods and products for modulating microbiota composition for improving the efficacy of a cancer treatment with an immune checkpoint blocker. MV and JMP were supported by La Ligue contre le cancer and ARC respectively. LZ received a special prize from the Swiss Bridge Foundation and ISREC. GK and LZ were supported by the Ligue Nationale contre le Cancer (Equipes labellisées), Agence Nationale pour la Recherche (ANR AUTOPH, ANR Emergence), European Commission (ArtForce), European Research Council Advanced Investigator Grant (to GK), Fondation pour la Recherche Médicale (FRM), Institut National du Cancer (INCa), Fondation de France, Cancéropôle Ile-de-France, Fondation Bettencourt-Schueller, Swiss Bridge Foundation, the LabEx Immuno-Oncology, the SIRIC Stratified Oncology Cell DNA Repair and Tumor Immune Elimination (SOCRATE); the SIRIC Cancer Research and Personalized Medicine (CARPEM), and the Paris Alliance of Cancer Research Institutes (PACRI). SM was supported by NIH (R01 CA161879 PI:SM). MC was supported by the Fondation pour la Recherche Médicale, the Fondation ARC pour la recherche sur le cancer and Institut Nationale du

Cancer. NW is a recipient of a Post-doctoral fellowship from the Agence Nationale de la Recherche. AS was supported by BMSI YIG 2014. FG is supported by SIgN core funding. LZ, MC, IGB are all sponsored by Association pour la Recherche contre le Cancer (PGA120140200851). FC was supported by INCA-DGOS (GOLD H78008). NC was supported by INCA-DGOS (GOLD study; 2012-1-RT-14-IGR-01). L'Oreal awarded a prize to MV. We are grateful to the staff of the animal facility of Gustave Roussy and Institut Pasteur. We thank P. Gonin, B. Ryffel, T. Angelique, N. Chanthapathet, H. Li and S. Zuberogoitia for technical help. LZ, MV and PL have filed patent applications n° EP 14190167 that relates to specific topic: Methods and products for modulating microbiota composition for improving the efficacy of a cancer treatment with an immune checkpoint blocker.

Authors' contribution: MV performed experiments and analyzed results represented in Fig. 1, 2C-D, 3A left panel, 4A-B and Supplemental Fig. 1B, 5CDE, 7, 8A, 9, 10, 12, 13C-E-F-G, 14B, 15, 16C, 17C, 21A-B, 22 and Supplemental Table 2 (alone or helped by RD + TY + NJ + SB + MPR + BR), JMP (helped by PO and VPC) assessed gut pathology and generated Fig 3A middle and right panels as well as Supplemental Fig. 2, 5A-B, 13D, 17, 18, 19 and 21C, CF + SR + MV did the experiments for Fig. 3D-E and Supplemental Fig. 11, SF (and EG) provided the patients specimen for the analyses of Fig. 3D-E and Supplemental Fig. 11, MC and NW performed the FISH analyses, Ki67, cCasp3 and MUC2 staining and qPCR experiments represented in Fig. 2A and Supplemental Fig. 4, 6, 8B-C. PL analyzed the 16S rRNA gene sequencing of mouse and human stools and described the PCA (Fig. 2C, Supplemental Fig.21A and Supplemental Table 1). SC and GE provided the tools and mice to analyze CTLA4 expression on gut T cells and ILCs represented in Supplemental Fig. 16A-B. AS and FG performed the flow cytometry analyses on LP DC subsets in Supplemental Fig. 13A-B. SM performed FITC dextran experiments depicted in Supplemental Fig. 3. CD, VPC and AR cultured the enteroids and studied the IEC-IEL cross talk represented in Fig. 2B. MPR and BR (helped by SB) performed experiments depicted in Fig. 4C and Supplemental Fig. 1A. MPR and SB executed and analyzed results of QPCR from FMT experiments represented in Fig. 4D-E and Supplemental Fig. 20 B-C. BR generated Supplemental Table 3 and 4 of patient characteristics. DR, MC, MB and IGB provided *il-10*, *nod2*, *il-10/nod2*, *tlr2* deficient mice as well as germ-free mice and bacterial species of interest (*Bf*, *Bt*, *E. coli*, *E. faecalis* *L. plantarum* for IGB and *Bc* for DR). PLW and EC characterized cultivable bacteria and performed mass spectrometry on bacterial species or isolates. JN purified PS and bacterial capsule materials. LZ, MV and JMP wrote the manuscript. CR, NC, CM and FC provided melanoma patients feces for FMT. GK and AE edited and critically reviewed the manuscript. LZ conceived the project and the experimental settings.

Materials & Methods

Patient and cohort characteristics. All clinical studies were conducted after informed consent of the patients, following the guidelines of the Declaration of Helsinki. Patient characteristics are detailed in Supplemental tables 3 and 4. Peripheral blood mononuclear cells (PBMC) were provided by Gustave Roussy Cancer Campus (Villejuif, France) and by the Department of Radiation Oncology (New York University [NYU], New York, NY, USA). Patients were

included from the following trials: Mel-Ipi-Rx (NCT01557114), and 2 Phase II trials at NYU combining ipilimumab with radiotherapy in either MM (NCT01689974) or NSCLC (NCT02221739). For memory T cell responses, blood samples were drawn from patients before and after 3 or 4 cycles of ipilimumab. High-throughput sequencing analyses (MiSeq Technology) of 16S rRNA gene amplicons in patients' feces pre-and post-injections of ipilimumab (V0, V1, V2, V3) were performed according to n° SC12-018; ID RCB: 2012-A01496-37 pilot study endpoints by GATC Biotech AG (Konstanz, Germany).

Clinical studies.

GOLD: Prospective immunomonitoring study of patients with MM receiving four injections of ipilimumab every three weeks. Feces were collected before each ipilimumab injection. Feces samples were frozen at -80°C and sent for 16S rRNA gene sequencing analysis at GATC Biotech AG (Konstanz, Germany).

MEL-IPI-RX: Phase I trial that combines ipilimumab and radiation therapy to assess the synergy between the two modalities. Dose escalation radiotherapy was administered with ipilimumab on week 1, 4, 7 and 10 weeks at 10mg/kg. Subsequently, a maintenance dose of ipilimumab was given every 12 weeks as long as the patient had a positive clinical response. Study code: NCT01557114.

MELANOMA ABSCOPAL TRIAL: Phase II randomized trial of ipilimumab versus ipilimumab plus radiotherapy in MM. Eligible patients had MM with at least 2 measurable sites of disease. All patients were randomly assigned to receive ipilimumab 3mg/kg i.v. versus ipilimumab 3 mg/kg i.v. plus fractionated radiotherapy to one of their measurable lesions. For patients assigned to the ipilimumab plus radiotherapy arm, ipilimumab treatment started after radiotherapy with a dose given on day 4 from the first radiotherapy fraction and repeated on days 25, 46, and 67. Response to treatment was evaluated at week 12 to assess clinical and radiographic responses in the non-irradiated measurable metastatic sites. Study code: NCT01689974.

NON-SMALL CELL LUNG CANCER ABSCOPAL TRIAL: Phase II study of combined ipilimumab and radiotherapy in metastatic non-small cell lung cancer (NSCLC). Eligible patients had chemo-refractory metastatic NSCLC with at least 2 measurable sites of disease. Patients received ipilimumab 3mg/kg i.v., within 24 hrs of starting fractionated radiotherapy. Ipilimumab

was repeated on days 22, 43, and 64. Patients were re-imaged between days 81-88 and evaluated for responses in the non-irradiated measurable metastatic sites. Study code: NCT02221739.

Mice. All animal experiments were carried out in compliance with French and European laws and regulations. Mice were used between 7 and 14 weeks of age. WT specific pathogen-free (SPF) C57BL/6J and BALB/c mice were obtained from Harlan (France) and Janvier (France), respectively, and were kept in SPF conditions at Gustave Roussy. C57BL/6 GF mice were obtained from Institut Pasteur and maintained in sterile isolators. *Il-10*^{-/-} C57BL/6 mice and WT C57BL/6 control animals were kindly provided by Anne O'Garra (National Institute for Medical Research, UK). *NOD2*^{-/-}, *Il10*^{-/-} and *NOD2*^{-/-}*Il10*^{-/-} mice (BALB/c background) were obtained from Institut Pasteur Lille. C57BL/6 *Tlr2*^{-/-} mice were provided by Ivo Gompers Boneca (Institut Pasteur, Paris, France), *Tlr4*^{-/-} mice were bred and maintained in the animal facility of Gustave Roussy, Villejuif, France.

Cell culture and reagents. OVA-expressing mouse fibrosarcoma MCA205 cells, murine colon carcinoma MC38 cells, RET melanoma model (a transgene-enforced expression of the *Ret* protooncogene under the control of the metallothionein-1 promoter driving spontaneous melanomagenesis, kindly provided by Viktor Umansky) (class I MHC H-2^b, syngeneic for C57BL/6 mice) and mouse colon carcinoma CT26 cells (class I MHC H-2^d, syngeneic for BALB/c mice) were cultured at 37°C under 5% CO₂ in RPMI-1640 medium supplemented with 10% heat-inactivated fetal bovine serum (FBS), 100 units/ml penicillin G sodium, 100 µg/ml streptomycin sulfate, 2mM L-glutamine, 1mM sodium pyruvate and non-essential amino acids (from this point on referred to as complete RPMI-1640; all reagents from Gibco-Invitrogen, Carlsbad, CA, USA). OVA-expressing MCA205 cells were selected in complete RPMI-1640 medium (as above) though supplemented with 50 µg/ml hygromycin B (Invitrogen, Life Technologies™).

Tumor challenge and treatment. Mice were subcutaneously injected into the right flank with 1×10^6 MCA205-OVA or MC38, with 0.5×10^6 RET or with 0.2×10^6 CT26 tumor cell lines. When tumors reached a size of 20 to 40 mm² (day 0), mice were injected intraperitoneally (i.p) with 100µg of anti-CTLA-4 mAb (clone 9D9) or isotype control (clone MPC11). Mice were

injected 5 times at 3-day intervals with 9D9, and tumor size was routinely monitored by means of a caliper. In order to evaluate the synergistic effect of vancomycin and anti-CTLA4, a prophylactic setting was established. In figure S21, anti-CTLA4 treatment started two days after tumor inoculation. In experiments using anti-IL-12p40 mAb (clone C17.8, 500 μ g per mouse) or anti-Ly6G mAb (clone 1A8, 200 μ g per mouse), mAbs (or their isotype controls, clone 2A3 in both cases) were injected i.p. every 2 days starting from day 0 until the final anti-CTLA-4 injection. Anti-ICOS mAb (clone 17G9) or isotype control mAb (clone LTF-2) were injected at 250 μ g per mouse, at the same times as for anti-CTLA4 mAb. In order to deplete CD4⁺ and CD8⁺ cells, clone GK1.5 and clone 53.72.1. or isotype control mAb were injected ip at 200 μ g/mice 4 days before anti-CTLA4 treatment. All mAbs for in vivo use were obtained from BioXcell (West Lebanon, NH, USA), using the recommended isotype control mAbs. The inhibitor of iNOS, N^G-monomethyl-L-arginine (L-NMMA; Sigma), was administered in PBS daily to mice i.p. at a dose of 2mg per mouse from the start of anti-CTLA4 treatment.

Antibiotic treatments. Mice were treated with antibiotics 2-3 weeks before tumor implantation and continued on antibiotics until the end of the experiment. A mix of ampicillin (1 mg/ml), streptomycin (5 mg/ml), and colistin (1 mg/ml) (Sigma-Aldrich), or vancomycin alone (0.25 mg/ml), or imipenem alone (0.25 mg/ml), or colistin alone (2.10³U/ml) were added in sterile drinking water. Solutions and bottles were changed 2-3 times a week, or daily for experiments with imipenem. Antibiotic activity was confirmed by macroscopic changes observed at the level of caecum (dilatation) and by cultivating the fecal pellets resuspended in BHI+15% glycerol at 0.1g/ml on blood agar plates for 48h at 37°C with in aerobic or anaerobic conditions.

Flow cytometry. Tumors, spleens and lymph nodes were harvested two days after the third injection of anti-CTLA-4 for antibiotics experiments or at the end of tumor growth (around day 20) for germ-free experiments. Excised tumors were cut into small pieces and digested in RPMI medium containing LiberaseTM at 25 μ g/ml (Roche) and DNase1 at 150UI/ml (Roche) for 30 minutes at 37°C. The mixture was subsequently passaged through a 100 μ m cell strainer. 2 \times 10⁶ splenocytes (after red blood cells lysis), lymph nodes or tumor cells were preincubated with purified anti-mouse CD16/CD32 (clone 93; eBioscience) for 15 minutes at 4°C, before membrane staining. For intracellular staining, the FoxP3 staining kit (eBioscience) was used.

Dead cells were excluded using the Live/Dead Fixable Yellow dead cell stain kit (Life Technologies™). Stained samples were run on a Canto II (BD Bioscience, San Jose, CA, USA) cytometer, and analyses were performed with FlowJo software (Tree Star, Ashland, OR, USA). For cytokine staining, cells were stimulated for 4 hrs at 37°C with 50ng/ml of phorbol 12-myristate 13-acetate (PMA; Calbiochem), 1µg/ml of ionomycin (Sigma), and BD Golgi STOP™ (BD Biosciences). Anti-CD45.2 (104), anti-FoxP3 (FJK-16s), anti-ICOS (7E17G9), anti-IFN-γ (XMG1.2), anti-TNF-α (MP6-XT22), anti-CXCR3 (CXCR3-173) and isotype controls rat IgG1 (eBRG1), IgG2a (eBRG2a), IgG2b (eBRG2b) were purchased from eBioscience. Anti-CD3 (145-2C11), anti-CD25 (PC61.5.3), KI67 (FITC mouse anti-human KI67 set), rat IgG1κ were obtained from BD Bioscience. Anti-CD4 (GK1.5), anti-CD8β (YTS1567.7), Rat IgG2a (RTK2758) were purchased from Biolegend (San Diego, CA, USA). Anti-CCR6 (140706) was obtained from R&D Systems, Minneapolis, MN. Eight-color flow cytometry analysis was performed with antibodies conjugated to fluorescein isothiocyanate, phycoerythrin, phycoerythrin cyanin 7, peridinin chlorophyll protein cyanin 5.5, allophycocyanin cyanin 7, pacific blue, or allophycocyanin. All cells were analyzed on a FACS CANTO II (BD) flow cytometer with FlowJo (Tree Star) software.

Microbial DNA extraction, 454 pyrosequencing and bacteria identification. Fecal samples used in this study were collected before or after one injection of anti-CTLA4 (or isotype control) from mice under vancomycin regimen or water, and were kept at -80°C until further analysis. Library preparation and sequencing were conducted at GATC Biotech AG (Konstanz, Germany). *Bacterial isolation, culture, and identification.* Fecal pellet contents were harvested and resuspended in BHI+15% glycerol at 0.1g/ml. Serial dilutions of feces were plated onto sheep's blood agar plates and incubated for 48h at 37°C with 5% CO₂ in aerobic or anaerobic conditions. After 48h, single colonies were isolated and Gram staining was performed. The identification of specific bacteria was accomplished through the combination of morphological tests and analysis by means of an Andromas MALDI-TOF mass spectrometer (Andromas, France).

Gut colonization with dedicated bacterial species. For inoculation of GF mice or mice treated with broad-spectrum antibiotics, colonization was performed the day following the first anti-CTLA4 injection by oral gavage with 100µl of suspension containing 1×10^9 bacteria. Efficient

colonization was checked by culture of feces 48h post oral gavage. *Bacteroides fragilis*, *Bacteroides thetaiotaomicron*, *Bacteroides distasonis*, *Bacteroides uniformis*, *Lactobacillus plantarum* and *Enterococcus hirae* were grown on blood agar plates (Biomérieux) for 48h at 37°C in anaerobic conditions. *E. coli* and *Burkholderia cepacia* were grown on blood agar plates for 24h at 37°C in aerobic conditions. Bacteria were harvested from the agar plates, suspended in sterile PBS, centrifuged and washed once with PBS, then resuspended in sterile PBS at an optical density (600nm) of 1, which corresponds approximately to 1×10^9 colony-forming units (CFU)/ml. In cases where more than one bacteria was administered, an equal volume of each bacteria suspension was mixed to give a suspension of equal proportion of each type of bacteria, to a total 1×10^9 bacteria/ml. For bacteria reconstitution experiments using mice previously treated with antibiotics, antibiotics treatment was stopped after 2-3 weeks at the first anti-CTLA4 injection, and mice were orally gavaged with 1×10^9 CFU the following day. *B. distasonis*, *B. uniformis*, *E. hirae*, and *E.coli* isolates used in the experiments were originally isolated from feces or mesenteric lymph nodes of SPF mice treated with anti-CTLA4 and identified as described above. *L. plantarum*, *B. fragilis* and *B. thetaiotaomicron* were provided by the Biobank of the Institut Pasteur, Paris, France. *Burkholderia cepacia* was kindly provided by the IUH Méditerranée Infection, Marseille, France (Supplemental Table 2). LPS-EK and LTA-SA (Invivogen) were administered by oral gavage, at a dose of 500µg per mouse.

TCR cross-linking assays. For cross-linking experiments, total cells isolated from draining or contralateral lymph nodes (after red blood cell lysis) were incubated in MaxiSorp plates (Nunc; 2×10^5 cells per well), precoated with anti-CD3 mAb (145-2C11) (0.5 µg per well; eBioscience). The supernatants were assayed at 48h by ELISA for mouse IFN-γ (BD).

Cytokine and antimicrobial peptide quantification. IL-12p70, IFN-γ (BD Biosciences) and IL-10 (R&D Systems, Minneapolis, MN), were measured by ELISA following the manufacturer's instructions. For quantification of lipocalin-2 from feces and caecum contents, individual (not pooled) samples were reconstituted in PBS containing 0.1% Tween 20 (at 100 mg/ml) and vortexed for 10-20 min to get a homogenous fecal suspension. These samples were then centrifuged for 10 min at 10,000 rpm. Clear supernatants were collected and stored at -20°C

until analysis. Lipocalin-2 levels were determined in the supernatants using the DuoSet murine Lcn-2 ELISA kit (R&D Systems, Minneapolis, MN) following the manufacturer's instructions.

FITC Dextran Assay to assess intestinal permeability. Mice were injected with either one dose or two doses of anti-CTLA4 or isotype control mAbs (administration as detailed above), and were water-starved overnight, 2 days following their last i.p. mAb administration. The following day, mice were orally administered with 0.44 mg/g body weight of a 100 mg/ml solution of FITC-dextran (FD4, Sigma) in PBS (pH 7.4). Four hrs later, blood was collected from each mouse by cardiac puncture. Blood was allowed to clot overnight at 4°C, then subsequently centrifuged at 3,000 rpm for 20 minutes to collect the serum. Dilutions of FITC-dextran in PBS, and separately in pooled mouse serum were used as a standard curve, with serum from mice not administered FITC-dextran used to determine the background. Absorbance of 100µl serum (diluted in PBS) was measured by microplate reader with excitation and emission filters set at 485 nm (20 nm band width) and 528 nm (20 nm band width), respectively (19). Experiments were performed at least twice, independently, with each read performed in duplicate.

Histology of gut tissue. The whole small intestine (duodenum, jejunum and ileum) and the colon were removed, cleaned from feces and fixed in 4% PFA for 2h. Rehydration of the tissue was performed in 15% sucrose for 1h and in 30% sucrose overnight. Small intestines or colons were cut longitudinally, with the resulting ribbons rolled, then embedded in optimum cutting temperature (OCT) compound (Sakura), snap frozen, and longitudinal 6 µm sections were prepared. For histological analysis, longitudinal sections were counterstained with hematoxylin and eosin. For histological quantitative analysis, inflammatory foci, appearance of the submucosa, length of villi, and the thickness of lamina propria were scored for each section by a pathologist. Score distribution between the groups were compared by proportional odds logistic regression using R software.

Intestinal MUC2 and Ki67 staining and evaluation. Intestinal tissue was fixed in freshly prepared Methacarn solution, subsequently incubated in methanol and toluene and embedded in paraffin. For immunohistochemistry, 5 µm-thick tissue sections were placed on Superfrost Plus

slides (Thermo Scientific), incubated for 10 min at 60° C and rehydrated through a series of graded alcohols and distilled water. Endogenous peroxidases were blocked by 3% hydrogen peroxide for 10 min. Antigen retrieval was performed in citrate buffer (10 mM, pH 6) by steaming sections in a microwave oven for 20 min. Tissue sections were blocked with 5% BSA/PBS for 30 min at RT and primary antibodies against MUC2 (1:200, sc15334, Santa Cruz Biotechnology) Ki67 (1:100, ab15580, Abcam) and Cleaved Caspase 3 (1:50, #9661, Cell Signaling Technology), were directly applied and incubated for 1 h at RT or overnight at 4°C, respectively. Slides were washed 3x in PBS and secondary antibody (1:200, UP511380, Interchim Uptima) was applied for 1 hour at RT. Targeted antigens were visualized by using 3,3'-diaminobenzidine solution (BD Pharmingen) followed by nuclear counterstain with hematoxylin. For immunofluorescence staining, staining procedure was done according to the protocol provided by Cell Signaling Technology. Primary antibody against MUC2 was used as indicated. Secondary antibody (1:200, A11008, Life Technologies) was applied for 1 hr at RT followed by nuclear counterstain with DAPI. Microscopic analyses were performed by using the Zeiss Axioptan 2 imaging microscope, Axio Imager Z1 microscope, Axiovision software (all from Zeiss, Oberkochen, Germany), and ImageJ software (20). Evaluation of MUC2- and Ki67-positive signals was performed by counting MUC2- and Ki-67-positive epithelial cells in all intact villi and/or crypts per tissue sections. Caspase 3 cleavage was assessed by calculating positively stained epithelial cells per mm² mucosal area. Thickness of pre-epithelial mucus layer in distal colon was obtained by calculating mean values of 10 distinct measurement points per tissue section.

Fluorescent in situ hybridization. Methacarn-fixed, paraffin-embedded colonic tissue sections (7 µm) were deparaffinized in toluene, washed in 95 % ethanol, and air-dried at RT. Tissue sections were incubated overnight (45°C) in hybridization buffer (20 mM Tris-HCl, 0.9 M NaCl, 0.1 % SDS, pH 7.4) containing Cy3-labeled bacterial probes EUB338 (5'-GCTGCCTCCCGTAGGAGT-3') and Bfra602 (5'-GAGCCGCAAACCTTTCACAA-3'), respectively, in a concentration of 5 ng/µl (21-23). Non-specific binding of probes was removed by subsequent incubation of slides in pre-warmed hybridization buffer and washing buffer (20 mM Tris-HCl, 0.9 M NaCl, pH 7.4), both for 15 min at 37°C. DAPI was used for nuclear counterstain and air-dried tissue sections were covered by using ProLongR Gold Antifade

reagent (Life Technologies). For combined mucus staining, anti-MUC2 antibody (1:100, sc15334, Santa Cruz Biotechnology) was applied for 15 min at RT, after a first wash step in hybridization buffer. Secondary antibody incubation (1:200, A11008, Life Technologies) including DAPI counterstain was performed for 15 min at RT. Tissue sections were washed in washing buffer for 5 min at RT and covered with antifade mounting medium. Microscopic analysis was performed by using the Axio Imager Z1 microscope and Axiovision software (all Zeiss).

Flow cytometry analyses of LP cell subsets. *Isolation of lamina propria cells from colon.* The whole colon was harvested and Peyer's patches were removed, as well as all fat residues and feces. Colons were cut longitudinally and then transversally into pieces of 1-2 cm length. After removing the intra-epithelial lymphocytes (IELs), the colon pieces were further cut into approximately 1mm squares, and incubated with 0.25 mg/ml collagenase VIII and 10 U/ml DNase I for 40 min at 37 °C with shaking, in order to isolate lamina propria cells (LPCs). After digestion, intestinal pieces were passaged through a 100µm cell strainer. For flow cytometry analysis, cell suspensions were subjected to a percoll gradient for 20 min, centrifuged at 2100 RPMI. Anti-mouse antibodies for CD45.2 (104), CD3 (145-2C11), CD4 (GK1.5), IFN-γ (XMG1.2), RORγt (AFKJS-9), anti-ICOS (7E17G9) were obtained from BioLegend, eBioscience and R&D. *CTLA4 staining on lamina propria cell subsets.* Large intestines were opened longitudinally, washed from feces and incubated on ice in PBS/EDTA (25 mM, without Ca²⁺/Mg²⁺, Gibco). Epithelial cells were removed by repeated rounds of shaking in PBS. Subsequently, the intestine was cut into small pieces and digested with Liberase TL (Roche) / DNaseI (Sigma) mix in DMEM (Gibco) at 37°C. Tissue was disrupted by pipetting and passing over a 100 µm mesh (BD). Homogenates were subjected to a 40/80 % Percoll (GE Healthcare) gradient. Lymphocytes were harvested from the interphase and stained with fixable Live/Dead stain Blue (Invitrogen) according to the manufacturer's instruction. Surface staining was performed with anti-CD3-PE-CF594 (145-2C11, BD), anti-CD4-HorizonV500 (RM4-5, BD), anti-CD19-BrilliantViolet650 (6D5, BioLegend), anti-Thy1.2-PerCp-eFluor710 (30-H12, eBioscience), anti-NKp46-biotin (polyclonal, R&D), Streptavidin-BrilliantViolet421 (BioLegend) and anti-CTLA-4-APC (UC10-4B9, eBioscience) or Armenian Hamster IgG Isotype Control APC (eBio299Arm, eBioscience). Cells were fixed with 4% PFA (Sigma) and

permeabilized and stained with 1x Perm buffer (eBioscience) and anti-Foxp3-PE (eBioscience), anti-GFP-Alexa488 (polyclonal, Molecular Probes) and CTLA-4-APC (UC10-4B9, eBioscience). Nonspecific binding was blocked with purified CD16/32 (93, eBioscience) and rat IgG (Dianova). Flow cytometry was performed on a Fortessa (BD) and data was analysed with FlowJo (TreeStar). *Analyses of DC subsets in anti-CTLA4 antibody-treated intestines.* Mesenteric lymph nodes were prepared by digestion with collagenase and DNase for 60 min and subsequently strained through a 70 μ m mesh. Colonic lymphocytes were isolated as previously described (24). In brief, colons were digested in PBS containing 5 mM EDTA and 2 mM DTT, with shaking at 37°C. After initial digestion, colonic tissue pieces were digested in collagenase/DNase containing RPMI medium for 30 min. Tissue pieces were further strained through a 70 μ m mesh. For flow cytometry analyses, cell suspensions were stained with antibodies against the following surface markers: CD11c (N418), CD11b (M1/70), MHC class II (M5/114.15.2), CD24 (M1/69), CD317 (ebio927), CD45 (30-F11), CD86 (GL1), CD40 (1C10). DAPI was used for dead cell exclusion. Antibodies were purchased from eBiosciences, BD Biosciences or BioLegend respectively. Cell populations were gated as follows: CD103⁺ DC (CD45⁺ CD11c⁺ MHC-II⁺ CD103⁺ CD24⁺), CD11b⁺ DC (CD45⁺ CD11c⁺ MHC-II⁺ CD11b⁺ CD24⁺), plasmacytoid DC (CD45⁺ CD11c⁺ MHC-II⁺ CD317⁺), mesenteric LNs (migratory fraction): CD103⁺ DC (CD45⁺ CD11c⁺ MHC-II⁺⁺ CD103⁺ CD24⁺), CD11b⁺ CD103⁺ DC (CD45⁺ CD11c⁺ MHC-II⁺⁺ CD103⁺ CD11b⁺ CD24⁺), CD11b⁺ DC (CD45⁺ CD11c⁺ MHC-II⁺⁺ CD11b⁺ CD24⁺), plasmacytoid DC (CD45⁺ CD11c⁺ MHC-II⁺ CD317⁺), mesenteric LNs (resident fraction): CD8 α ⁺ DC (CD45⁺ CD11c⁺ MHC-II⁺ CD24⁺ CD11b⁻), CD11b⁺ DC (CD45⁺ CD11c⁺ MHC-II⁺ CD11b⁺).

Preparation of capsular polysaccharide-enriched fractions. Fractions containing capsular polysaccharides were prepared as previously described (25). Briefly, bacteria were extracted twice by a hot 75% phenol/water mixture for 1h at 80°C. After centrifugation at 1000 g for 20 min, water phases were pooled and extracted with an equivalent volume of ether. Water phases were then extensively dialyzed against water and lyophilized. Extracted compounds were subsequently submitted to digestion by DNAase, RNAase, α -chymotrypsin, Streptomyces griseus proteases and trypsin. The digested solutions were dialysed against water and dried, resulting in fractions enriched in capsular polysaccharides. Quantification of LPS content. The

presence of LPS in capsular polysaccharide-enriched fractions was investigated using the HEK-Blue™ TLR4 cell line (Invivogen, Toulouse), a derivative of HEK293 cells that stably expresses the human TLR4, MD2 and CD14 genes along with a NF-κB-inducible reporter system (secreted alkaline phosphatase). Cells were used according to the manufacturer's instructions. The different capsular polysaccharide-enriched fractions were added at concentrations ranging from 1 ng to 10 µg/ml in 96-wells plates and cells were then distributed at 5×10^4 per well in 200 µl DMEM culture medium. Alkaline phosphatase activity in the culture supernatant was measured after 18h. LPS content was determined by TLR4 signaling activation by comparison with a standard curve obtained using ultrapure LPS from *E. coli* K12 (Invivogen, Toulouse). The LPS content in the PS *B. fragilis* fraction was estimated at 1.4 pg/ µg of PS. The LPS residual content in the PS *B. fragilis* fraction could not account for its activity, as confirmed by the lack of bioactivity observed by adding LPS to the polysaccharide capsular fractions of *B. distasonis* compared to its effect in the absence of LPS.

Monosaccharide analysis of the capsular polysaccharide-enriched fractions from *B. fragilis* and *B. distasonis* Monosaccharides were analyzed after total hydrolysis of 10 µg of capsular polysaccharide-enriched fraction by 2N TFA at 110°C for 2 hrs. They were detected by capillary electrophoresis monitored by laser-induced fluorescence (CE-LIF) using a 20 mM sodium borate buffer after re-N-acetylation and derivatization by the fluorescent probe 8-Aminopyrene-1,3,6-Trisulfonate (26, 27). Galacturonic acid, Fucose, Galactose and N-Acetyl-amino sugars (N-Acetyl-Glucosamine, N-Acetyl-Galactosamine and N-Acetyl-Quinovosamine) were detected, in agreement with the composition of *B. fragilis* capsular polysaccharides described in Pantosti et al (25) and Bauman et al (28).

Assessing CD4⁺ T cell memory responses. Murine systems. Bone marrow-derived dendritic cells (BM-DCs) were generated from femurs and tibiae of C57BL/6 mice, cultured for 7 days in Iscove's medium (Sigma-Aldrich) with J558 supernatant (final GM-CSF concentration of 40 ng/ml), 10% FCS, 100 IU/ml penicillin/streptomycin, 2 mM L-glutamine, 50 µM 2-mercaptoethanol (Sigma-Aldrich) and split every 3-4 days. At day 7, BM-DCs were infected with the isolated bacterial strains at multiplicity of infection (MOI) of 10 or 50, for 1h at 37°C in complete Iscove's medium without antibiotics, onto specific low binding 6 wells plates (Sigma).

Cells were then washed with PBS and incubated in complete Iscove's medium supplemented with gentamicin (50µg/ml) to kill extracellular bacteria. For *Burkholderia cepacia*, the antibiotic meropenem (2µg/mL, Astra Zeneca) was required. After 24h, BM-DCs were cultured together with CD4⁺ T cells purified from the spleens of mice that had received 7 days treatment of anti-CTLA4 mAb (i.e 3 anti-CTLA4 mAb injections, as detailed above) in complete RPMI medium. CD4⁺ T cells were isolated by depletion of non CD4⁺ T cells using a cocktail of biotin-conjugated antibodies against CD8α, CD11b, CD11c, CD19, CD45R (B220), CD49b (DX5), CD105, MHC-class II, Ter-119 and TCRγδ as primary labeling reagent. The cells were then magnetically labeled with anti-biotin MicroBeads (Miltenyi Biotec, France). The magnetically labeled non-target cells were depleted by retaining them on an Automacs Separator, while the unlabeled target cells passed through the column. Co-cultures were set up at a ratio of 1 DC to 2 CD4⁺ T cells. We confirmed by flow cytometry that over 95% of magnetic-sorted cells were CD4⁺ T cells. Co-culture supernatants were collected at 24h, and assayed for IL-10 and IFN-γ using commercial ELISA. *Recall of human CD4⁺ T cell responses directed against commensals.* Frozen PBMC before and/or after ipilimumab therapy were thawed, washed and resuspended in the recommended separation medium (PBS, 1mM EDTA, 2% human AB⁺ serum (Jacques Boy); STEMCELL Technologies) for magnetic bead separation. Monocytes were enriched from 2 × 10⁶ PBMC (EasySep™ Human Monocyte Enrichment Kit, STEMCELL Technologies) and resuspended in RPMI-1640 (GIBCO Invitrogen), 10% human AB⁺ serum supplemented with 1% 2 mmol/L glutamine (GIBCO Invitrogen), and GM-CSF (1000UI/mL, Miltenyi), without any antibiotics. Monocytes were seeded in 96-well round bottom plates at 5 × 10³ cells/well either alone, in the presence of one of the five selected bacterial strains (Table 2) at a multiplicity of infection (MOI) of 100, or with LPS as positive control (1µg/mL, Sigma) plus sCD40L (1µg/mL, Miltenyi) and incubated for 1 hour at 37°C, 5% CO₂. During incubation, the remaining autologous PBMC fractions were enriched for memory CD4⁺ T cells (EasySep™ Human Memory CD4 Enrichment Kit, STEMCELL Technologies). The enriched CD4⁺CD45RO⁺ T cells were washed, counted and resuspended at 5 × 10⁴/well in RPMI-1640, 10% human AB⁺ serum, 1% 2 mmol/L glutamine, 20UI/mL IL-2 (Proleukine) either with 1% penicillin/streptomycin (PEST; GIBCO Invitrogen) and 50µg/ml of gentamycin (GIBCO Invitrogen) or with meropenem antibiotic for *Burkholderia cepacia* (2µg/mL, Astra Zeneca). CD4⁺CD45RO⁺ T cells were also incubated alone, or with CD3/CD28 beads (1µL/mL,

Deanabeads T-Activator, Invitrogen) as a positive control. Monocyte-bacteria/CD4⁺CD45RO⁺ T cell co-cultures were incubated for 48 hrs at 37°C, 5% CO₂. Monocytes and memory CD4⁺CD45RO⁺ T cell enrichment were confirmed as being >98% purity by flow cytometry. Supernatants were harvested, cleared by centrifugation (1200rpm, 5 min) and stored at -20°C for determination of IFN- γ or IL-10, as measured by commercial ELISA or Luminex MagPix technology (Biorad).

Adoptive cell transfer. CD4⁺ T cells were isolated from co-culture with DCs that had been pulsed with bacteria at a MOI of 10, as described above. 1×10^6 CD4⁺ T cells were adoptively transferred i.v into GF or ACS treated mice, one day after the first anti-CTLA4 mAb injection. Mice were injected with anti-CTLA4 mAb and tumor sizes were monitored as detailed previously. After 24h of coculture with bacteria as described above, BM-DCs were removed from low binding plates, washed, and counted. Alternatively to bacteria infection, BM-DC were pulsed with peptides (KD)₂₀ synthesized by Smartox Biotechnology (Gillonay, France) or with capsular polysaccharide-enriched fractions (final concentration of 10 μ g/ml). One million DC were adoptively transferred i.v into antibiotics -treated mice one day after the first anti-CTLA4 mAb injection. Mice were administered with anti-CTLA4 mAb and tumor sizes were monitored as detailed above.

Small intestine crypt isolation and organoid culture. Crypt isolation and organoid culture was performed as previously described (29) with the following modifications. Briefly, the ileum of 10-13 week old mice were cut longitudinally and scraped with a cover slip to remove villi. The intestine was cut transversely into 2-4 mm pieces and washed 4 times with cold PBS. Fragments were then incubated in 2 mM EDTA in PBS for 30 minutes on ice. Following the removal of EDTA medium, fragments were vigorously resuspended in PBS containing 10% FCS (Gibco) and passed through a 70 μ m strainer (BD Bioscience). This step was repeated 3 times. Isolated crypts were pelleted and washed in Advanced DMEM/F12 (ADF) (Invitrogen). Crypts were then resuspended in 1mL of Matrigel growth factor reduced basement membrane matrix (Corning) and 50 μ L drops were placed into pre-warmed 24-well plates. Following Matrigel polymerisation, crypts were overlaid with ADF supplemented with 100 U/mL penicillin G sodium, 100 μ g/mL streptomycin sulphate, 2 mM L-glutamine, 10 mM HEPES, 1x N2

supplement, 1x B27 supplement, 50 ng/mL mEGF, 100 ng/mL mNoggin (Peprotech, Hamburg, Germany), *N*-acetylcysteine (Sigma) (reagents from Invitrogen unless otherwise indicated) and 10% conditioned medium of R-Spondin-1 transfected HEK 293T cells. Media was changed every 2-3 days. Cultures were split every 7-10 days by first dissolving the matrigel with cold ADF and mechanically disrupting the organoids using a narrowed Pasteur pipette.

Intraepithelial lymphocyte isolation. The ileum and colon of 8-12 week old mice were harvested. Following the removal of Peyer's patches, mesenteric fat and feces, the intestine was cut longitudinally and then transversely into small pieces. Fragments were then transferred to 50 mL conical tubes, vortexed and shaken for 30 minutes at 37°C in PBS containing 5% FCS, 5 mM EDTA and 1 mM DTT. The suspension was then passed through a 100 µM cell strainer (BD) and pelleted by centrifugation. Fragments remaining on the cell strainer were collected digested again. Cell pellets were resuspended in RPMI containing 10% FCS.

Culture of organoids with IELs and TLR agonists. TLR agonists (1.3 µg/mL LTA-SA, 1.3 µg/mL LPS, 0.13 µg/mL of Flagellin (from Invivogen), 0.13 µg/mL Poly IC (Ampligen)) were added to organoid cultures on the day of splitting. Twenty-four hours later, IELs isolated from isotype control or 9D9 treated mice were added to organoid cultures. Seventy two hours later, organoids embedded in matrigel were formalin fixed and stained for caspase 3 expression.

Formalin-fixed paraffin-embedded blocks (FFPE) of organoids. Organoids derived from the ileum of mice were fixed in 10% neutral buffered formalin for 4h. Organoids were then transferred to Mini-Micro Flow cassettes, paraffin embedded with a Tissue-Tek® VIP® 6 Vacuum Infiltration Processor (Sakura) and cut into 3µm-thick sections.

Immunohistochemistry staining of Cleaved Caspase 3 expression. FFPE organoids sections were deparaffinised and rehydrated through a series of graded alcohols and distilled water. Antigen retrieval was performed by pre-treating sections with 0.01 M sodium citrate buffer (pH 6.0, Diapath) for 30 min in a 98°C water bath. Endogenous peroxidase activity was inhibited by treating sections with 3% hydrogen peroxidase (#S202386, DAKO) for 10 min. Sections were blocked with IHC/ISH Super Blocking (#PV6122, LeicaBiosystem) for 10 min. The primary

polyclonal Rabbit antibody (Ab), Cleaved Caspase-3 (Asp175) (#9661, Cell Signalling, 1µg/mL) was incubated for 1h, followed by the secondary Ab, PowerVision Poly-HRP anti-Rabbit IHC Detection Systems (#PV6114, LeicaBiosystem) for 20 minutes. Peroxidases were detected with Di Amino Benzidine-peroxidase substrate kit (DAKO), and counterstained with Mayer's haematoxylin.

Counting of cleaved Caspase 3 positive cells. At 400X magnification in all fields, cleaved Caspase 3 positive cells and the total number of cells were counted on 2 levels for each condition. Counting was replicated at least twice.

Gene expression analysis. Total RNA was extracted by using the column-based RNeasy Mini Kit (Qiagen). Complementary DNA was generated by using the AffinityScript QPCR cDNA Synthesis Kit (Agilent Technologies) according to the manufacturer's instructions. Quantification of gene expression was performed on Stratagene™ Mx3005P by using the Brilliant III Ultra-Fast SYBR® Green QPCR Master Mix (both Agilent Technologies) and gene-specific primers for β-ACTIN for_5'-GAATGGGTCAGAAGGACTCCTATG-3', rev_5'-CCATGTCGTCCCAGTTGGTAA-3', CTLA4 for_5'- TCACTGCTGTTTCTTTGAGCA-3', rev_5'-GGCTGAAATTGCTTTTCACAT-3', IL17A for_5'-ACCGCAATGAAGACCCTGATA-3', rev_5'- GCACTGAGCTTCCCAGAT-3', IL17F for_5'-ATTCCAGAACCGCTCCAGTTC-3', rev_5'-GGTCTCGAGTGATGTTGTAATCC-3', IFNγ for_5'-GCTTTGCAGCTCTTCCTCAT-3', rev_5'-CCAGTTCCTCCAGATATCCAAG-3', IDO1 for_5'-GGGCTTTGCTCTACCACATC-3', rev_5'-AAGGACCCAGGGGCTGTAT-3', IFIT2 for_5'- CAATGCTTAGGGGAAGCTGA-3', rev_5'-TGATTTCTACTTGGTCAGGATGC-3', IFI44 for_5'-CTGATTACAAAAGAAGACATGACAGAC-3', rev_5'-AGGCAAAACCAAAGACTCCA-3', Usp18 for_5'-GCCCACGTTGGGATGGCTGA-3', rev_5'-ATAGGCCGTTTCCC GCCAGC-3', IL6 for_5'-ACACATGTTCTCTGGGAAATCGT-3', rev_5'-AAGTGCATCATCGTTGTTTCATACA-3', and Reg3β for_5'-ATGCTGCTCTCCTGCCTGATG-3', rev_5'-CTAATGCGTGCGGAGGGTATATTC-3' (Eurogentec).

FMT experiments. Germ-free adult female C57BL/6J mice were obtained from CDTA (Orleans, France) and Institut Pasteur (Paris, France). Fecal samples from GOLD cohort were frozen after being homogenised with brain-heart-infusion media (BHI) supplemented with 15% glycerol (0.1g/ml) and stored immediately at -80°C . FMT was performed by thawing the fecal material and 0.2 ml of the suspension was transferred by oral gavage into each germ-free recipient. In addition another 0.1ml was applied on the fur of each animal. Mice were subsequently maintained in a gnotobiotic isolator with irradiated food and autoclaved water in our animal facility (Plateforme Evaluation Préclinique, Villejuif, France). Two weeks after microbiota transfer, MCA205-OVA tumor cells were injected subcutaneously and mice were treated with anti-CTLA4 mAb or isotype control as previously described.

Quantification of bacteria by q-PCR. Genomic DNA was isolated from fecal samples using the QIAamp DNA Stool Mini Kit (Qiagen) following the manufacturer's instructions. Targeted qPCR systems were applied using either Taqman technology (for systems targeting All Bacteria domain and Bacteroidetes/Prevotella group or SybrGreen for different Bacteroides species.

The following primers and probes were used:

| Target group | PCR System | Primers and probes | Oligo sequence 5'-3' | Ref |
|---|------------|--------------------|---|-------------|
| All bacteria (universal 16S rDNA) | TaqMan | Forward | CGGTGAATACGTTCCCGG | (30, 31) |
| | | Reverse | TACGGCTACCTTGTTACGACTT | |
| | | Probe | 6 FAM -CTT GTA CAC ACC GCC CGT C-MGB | |
| Bacteroides/ Prevotella | TaqMan | Forward | CCTWCGATGGATAGTGGTT | (30) |
| | | Reverse | CACGCTACTTGGCTGGTTCAG | |
| | | Probe | VIC- AAG GTC CCC CAC ATT G -MGB | (32) |
| <i>B. fragilis</i> | SybrGreen | Forward | TGATTCCGCATGGTTTCATT | (33) |
| | | Reverse | CGACCCATAGAGCCTTCATC | |
| <i>B. thetaiotaomicron</i> | SybrGreen | Forward | GGTAGTCCACACAGTAAACGATGAA | (34) |
| | | Reverse | CCCGTCAATTCCTTTGAGTTTC | |

| | | | | |
|----------------------|-----------|---------|-------------------------|------|
| <i>B. uniformis</i> | SybrGreen | Forward | TCTTCCGCATGGTAGAACTATTA | (35) |
| | | Reverse | ACCGTGTCTCAGTTCCAATGTG | |
| <i>B. distasonis</i> | SybrGreen | Forward | TGCCTATCAGAGGGGGATAAC | (35) |
| | | Reverse | GCAAATATTCCCATGCGGGAT | |

Quantitative-PCR was carried out using a ABI PRISM 7300 quantitative PCR System with software version 1.2.3 (Applied Biosystem). Amplification and detection were carried out with either TaqMan Universal PCR MasterMix or SYBRGreen PCR Master Mix (Applied-Biosystems) in a final volume of 25 μ l containing a final concentration of 0.2 μ M for primers and probes and 25 μ g of DNA templates. Amplifications were carried out using the following ramping profile: 1 cycle at 95 °C for 10 min, followed by 40 cycles of 95°C for 30 s, 60°C for 1 min. For SYBR-Green amplification, a melting step was added. Quantitative-PCR data were normalized to the expression levels of total bacteria by means of the $2^{-\Delta C_t}$ method.

Statistical analyses. Data were analyzed with Microsoft Excel (Microsoft Co., Redmont, WA, USA), Prism 5 (GraphPad, San Diego, CA, USA), and R. Data are presented as means \pm SEM and *p*-values computed by paired or unpaired *t*-tests where applicable. Tumor growth was subjected to a linear mixed effect modeling applied to log pre-processed tumor surfaces. The *p*-values were calculated by testing jointly whether both tumor growth slopes and intercepts (on a log scale) were dissimilar between treatment groups of interests. All reported tests are two-tailed and were considered significant at *p*-values < 0.05. Statistical analyses pertaining to 16S rRNA gene amplicons sequencing are detailed in Figure legends.

Supplemental References

19. M. Venkatesh *et al.*, Symbiotic bacterial metabolites regulate gastrointestinal barrier function via the xenobiotic sensor PXR and Toll-like receptor 4. *Immunity* **41**, 296 (Aug 21, 2014).
20. C. A. Schneider, W. S. Rasband, K. W. Eliceiri, NIH Image to ImageJ: 25 years of image analysis. *Nature methods* **9**, 671 (Jul, 2012).
21. R. I. Amann *et al.*, Combination of 16S rRNA-targeted oligonucleotide probes with flow cytometry for analyzing mixed microbial populations. *Applied and environmental microbiology* **56**, 1919 (Jun, 1990).

22. A. H. Franks *et al.*, Variations of bacterial populations in human feces measured by fluorescent in situ hybridization with group-specific 16S rRNA-targeted oligonucleotide probes. *Applied and environmental microbiology* **64**, 3336 (Sep, 1998).
23. L. Rigottier-Gois, V. Rochet, N. Garrec, A. Suau, J. Dore, Enumeration of Bacteroides species in human faeces by fluorescent in situ hybridisation combined with flow cytometry using 16S rRNA probes. *Systematic and applied microbiology* **26**, 110 (Mar, 2003).
24. A. Schlitzer *et al.*, IRF4 transcription factor-dependent CD11b+ dendritic cells in human and mouse control mucosal IL-17 cytokine responses. *Immunity* **38**, 970 (May 23, 2013).
25. A. Pantosti, A. O. Tzianabos, A. B. Onderdonk, D. L. Kasper, Immunochemical characterization of two surface polysaccharides of Bacteroides fragilis. *Infect Immun* **59**, 2075 (Jun, 1991).
26. F. T. Chen, T. S. Dobashi, R. A. Evangelista, Quantitative analysis of sugar constituents of glycoproteins by capillary electrophoresis. *Glycobiology* **8**, 1045 (Nov, 1998).
27. J. Nigou, A. Vercellone, G. Puzo, New structural insights into the molecular deciphering of mycobacterial lipoglycan binding to C-type lectins: lipoarabinomannan glycoform characterization and quantification by capillary electrophoresis at the subnanomole level. *Journal of molecular biology* **299**, 1353 (Jun 23, 2000).
28. H. Baumann, A. O. Tzianabos, J. R. Brisson, D. L. Kasper, H. J. Jennings, Structural elucidation of two capsular polysaccharides from one strain of Bacteroides fragilis using high-resolution NMR spectroscopy. *Biochemistry* **31**, 4081 (Apr 28, 1992).
29. T. Sato *et al.*, Single Lgr5 stem cells build crypt-villus structures in vitro without a mesenchymal niche. *Nature* **459**, 262 (May 14, 2009).
30. J. P. Furet *et al.*, Comparative assessment of human and farm animal faecal microbiota using real-time quantitative PCR. *FEMS microbiology ecology* **68**, 351 (Jun, 2009).
31. M. T. Suzuki, L. T. Taylor, E. F. DeLong, Quantitative analysis of small-subunit rRNA genes in mixed microbial populations via 5'-nuclease assays. *Applied and environmental microbiology* **66**, 4605 (Nov, 2000).
32. W. Manz, R. Amann, W. Ludwig, M. Vancanneyt, K. H. Schleifer, Application of a suite of 16S rRNA-specific oligonucleotide probes designed to investigate bacteria of the phylum cytophaga-flavobacter-bacteroides in the natural environment. *Microbiology* **142 (Pt 5)**, 1097 (May, 1996).
33. T. Odamaki *et al.*, Distribution of different species of the Bacteroides fragilis group in individuals with Japanese cedar pollinosis. *Applied and environmental microbiology* **74**, 6814 (Nov, 2008).
34. S. M. Lee *et al.*, Bacterial colonization factors control specificity and stability of the gut microbiota. *Nature* **501**, 426 (Sep 19, 2013).
35. J. Tong, C. Liu, P. Summanen, H. Xu, S. M. Finegold, Application of quantitative real-time PCR for rapid identification of Bacteroides fragilis group and related organisms in human wound samples. *Anaerobe* **17**, 64 (Apr, 2011).

Supplemental Figure legends

Supplementary Figure 1. The gut microbiota is implicated in the immunostimulatory properties of anti-CTLA4 mAb in the MC38 colon carcinoma model. **A-B.** *Effects of ATBx in the efficacy of CTLA4 blockade against transplantable colon and melanoma cancers.* One representative graph out of two independently performed experiments (n = 5 per group) is depicted. C57BL/6 mice previously fed with antibiotics or water as control, in the drinking water to deplete gut microbiota were implanted s.c. with Ret melanoma cells. Mice were subsequently treated with anti-CTLA4 or isotype control mAbs, when implanted tumors were palpable, and tumor growth was followed over 20 days. **B.** *Idem* as A. with colon carcinoma cells. **C-D.** *Effects of oral antibiotics on the immunostimulatory activity of anti-CTLA4 Ab.* **C.** Flow cytometric analyses of ICOS expression on effector CD4⁺Foxp3⁻ T cells harvested from the spleen at 20 days after the first administration of 9D9 or Iso Ctrl Ab. **D.** CD3⁺ T cells among CD45⁺ tumor infiltrating cells harvested two days after the third administration of 9D9 or Iso Ctrl Ab. **E.** The percentages of CD4⁺Foxp3⁺ Tregs in the tumor and in the spleens of mice treated or not with antibiotics is depicted (left and middle panels respectively), as well as the percentage of ICOS⁺ Tregs splenocytes (right panel). Three experiments comprising 5 mice/group are pooled, each dot representing one mouse. Data were analysed by one-way ANOVA with Bonferroni's multiple comparison test. * $p < 0.05$, ** $p < 0.01$, *** $p < 0.001$, ns = not significant.

Supplementary Figure 2. Hallmarks of intestinal pathology observed in α CTLA4-treated mice are dependent upon intestinal microbiota. Small intestines and colons were taken and processed for histopathological scoring (as detailed in the Materials & Methods) from MCA205 tumor-bearing specific pathogen free (SPF) mice 8 days after beginning α CTLA4 (or isotype control) mAb therapy as detailed before (i.e. after 3 mAb injections). Neither weight loss nor intestinal bleeding were observed after 3 intraperitoneal injections of anti-CTLA4 (not shown). The length of small intestine villi (**A**) and the height of the mucosa of colons (**B**) were measured from at least 8 distinct regions from each mouse. In an additional experiment, the colon mucosal height was measured in the same way in SPF and germ-free mice (**C**), 23 days following the beginning of mAb treatment. Length of the villi and mucosae height of the colon were significantly reduced following CTLA4 blockade (Supplemental Fig. 2A-B) in mice reared in SPF conditions, but less so in GF mice. (**D**) The level of colitis was scored for mice treated or not with antibiotics receiving anti-CTLA4 or isotype control Ab. Data shown are from one of 2 independent experiments (n = 5 per group) and depict the mean \pm SEM. *** $p < 0.001$, * $p < 0.05$ by unpaired two-tailed *t*-test (A & B); ** $p < 0.01$, ns = not significant by one-way ANOVA with Bonferroni's multiple comparison test (C). Score distributions between groups were compared by proportional odds logistic regression, ** $p < 0.01$, ns = not significant (D).

Supplementary Figure 3. Intestinal permeability is not disrupted following CTLA4 blockade in vivo. C57BL/6 mice were administered either anti-CTLA4 or isotype control mAbs from when implanted tumors reached 25mm² in size. Two days later, mice were water-starved overnight, and the following day (day 3 post mAb dosing), mice were orally administered FITC-dextran. After 4 hours, blood was collected from each mouse by cardiac puncture and the blood concentration of FITC-dextran was determined (**A**). The same procedure was carried out in a

separate group of mice that had received two anti-CTLA4 (or isotype control) mAb doses (**B**). Data depict the mean \pm SEM. ns = not significant by unpaired two-tailed *t*-test.

Supplementary Figure 4. Mucus staining and goblet cells of the intestines are not markedly affected by anti-CTLA4 therapy. SPF C57BL/6 mice were treated as previously detailed with isotype control or anti-CTLA4 mAb. Two days post therapy, Muc2⁺ intestinal epithelial cells (IECs) were counted per crypt in the ileum and the colon following immunofluorescence staining (**A**). The length of the mucus layer of the colon was measured at the same timepoint (**B**). Data depict the mean \pm standard deviation. ns = not significant by unpaired two-tailed *t*-test.

Supplementary Figure 5. Dynamic changes of lymphocyte subsets in the colonic lamina propria and lipocalin-2 levels. A.B. *Lipocalin-2 levels are increased in the stools and caeca of anti-CTLA4-treated mice.* MCA205 tumor-bearing mice were administered either α CTLA4 or the appropriate isotype control mAb, every 3 days, from when the implanted tumors reached 25mm² in size. Stools were collected throughout the timecourse of mAb treatment for subsequent lipocalin-2 (Lcn2) ELISA (**A**). Eight days after the beginning of mAb administration (i.e. after 3 mAb injections), the contents of caeca were collected for measurement of Lcn-2 by ELISA (**B**). In separate groups of mice, Arrows in **A** indicate the times of mAb administration. Data in **A** and **B** are pooled from 4 independent experiments (*n* = 5 per group) and depict the mean \pm SEM. ** *p* < 0.01 by unpaired two-tailed *t*-test. **C.E.** C57BL/6 mice were administered either anti-CTLA4 or the appropriate isotype control mAb every 3 days as detailed before. After 3 mAb injections (day 8 post start of treatment), colonic lymphocytes were isolated and the percentages of ROR γ t⁺ γ δ T cells (**C**), ROR γ t⁺ CD4⁺ T cells (**D**) and IFN- γ ⁺ CD4⁺ T cells (**E**) were determined by flow cytometry. Data depict the mean \pm SEM at least three independently performed experiments that have been pooled. ** *p* < 0.01, * *p* < 0.05, ns = not significant, by unpaired two-tailed *t*-test.

Supplementary Figure 6. Rapid proliferation and immune activation of the intestinal epithelial layer 24 hrs post-CTLA4 blockade. SPF C57BL/6 mice or RegIII β ^{-/-} mice were treated as previously detailed with isotype control or anti-CTLA4 mAb. 24hrs post mAb therapy, Ki67⁺ intestinal epithelial cells (IECs) were counted per crypt in the ileum and the colon following immunofluorescence staining as shown in the micrographs in the top panels, and quantified beneath (**A**). **B-E** depict total distal ileum biopsy gene expression levels at 24hrs post treatment with 9D9 Ab therapy by qPCR analysis. Data depict the mean \pm standard deviation of two experiments. *** *p* < 0.001, ** *p* < 0.01, * *p* < 0.05, by Mann-Whitney non-parametric test or *t*-test. ns = not significant by unpaired two-tailed *t*-test.

Supplementary Figure 7. Trend towards a decrease of Bacteroidales in feces 24 hrs post-anti-CTLA4 Ab. QPCR analyses using specific probes targeting Bacteroidales and two distinct *Bacteroides* species in feces (**A**) or in colon mucosae (**B**) performed at 24-48 hrs post-anti-CTLA4 or isotype control Ab, in complementation to Fig. 2D. Each dot represents one mouse in two gathered experiments. Student *t*' test : **p* < 0.05, ns = not significant.

Supplementary Figure 8. Localisation of *B. fragilis* in the mucosal layer between lumen and epithelium of the colon. *A. Antitumor efficacy of Bf in GF mice treated with CTLA4 blockade.* Oral feeding of tumor bearing-mice reared in SPF (left panel) and GF conditions with or without

Bf. Tumor sizes are depicted from 3 experiments (right panel) and are shown at day 15 post-9D9 or Iso Ctrl Ab-treatment. A representative tumor growth is depicted in the main Fig. 4B. B. Examples of histological evaluation of bacteria in the colon using fluorescence *in-situ* hybridisation for all bacterial species (eub338 probe; **B**) and *B. fragilis* (Bfra0602 probe; **C**), with another area of the latter magnified to visualise *B. fragilis* (right panels), in germ-free mice monoassociated with *B. fragilis* (upper panels) or germ-free mice as controls (lower panels). Pictures shown are from the middle part of the colon taken from C57BL/6 mice 1 day post one administration of anti-CTLA4 or isotype control mAbs ($n = 6$). Scale bar: 50 μ m or 10 μ m, T=tissue, M=inner mucus layer, L=lumen.

Supplementary Figure 9. *B. fragilis* induces Th1 responses in tumor draining lymph nodes.

A. Oral feeding of tumor bearing-mice reared in GF conditions with or without *B. fragilis*. Tumor draining-and contralateral lymph nodes were harvested at day 20 post-tumor inoculation and stimulated with anti-CD3 Ab for 48 hrs. IFN γ concentrations were monitored in culture supernatants using commercial ELISA. Means \pm SEM of IFN γ release for 5 mice/group are shown. Anova statistical analyses: * p <0.05, ** p <0.01, *** p <0.001, ns: not significant. **B.** Flow cytometry determination of CD80 expression on CD11c⁺I-A^bCD45⁺ tumor infiltrating cells in one representative experiment out of two yielding similar results. Student t'test: * p <0.05.

Supplementary Figure 10. IL-10 release by memory T cell splenocytes exposed to *Bacteroides* species after CTLA4 blockade.

Same experimental setting as that described in Fig. 3C monitoring IL-10 in ELISA from supernatants of mixed cocultures of BM-DC and CD4⁺ T cells with *Bacteroides* spp. Memory Th1 responses characterized by interferon (IFN)- γ production were observed against *Bf* and *Bt* (but not *B. distasonis* or *B. uniformis*), with little concomitant IL-10 production, mainly in splenocytes from anti-CTLA4 -treated mice (Fig. 3C).

Supplementary Figure 11. Selective restoration of T cell unresponsiveness to *B. fragilis* and *B. thetaiotaomicron* in advanced cancer patients with ipilimumab.

Circulating memory Th1 and Tr1 T cell responses against some *Bacteroides* spp. and other commensals prior to and after at least 2 administrations of ipilimumab, given as a standalone therapy or combined with local radiotherapy (Supplemental Table 3) in advanced metastatic melanoma (MM) and non small cell lung cancer (NSCLC) patients. CD4⁺CD45RO⁺ T cells from PBMC of 11 healthy volunteers or 27 advanced (11 melanoma and 6 NSCLC cancer) patients before and after at least 2 injections of ipilimumab were restimulated with autologous CD14⁺ cells (sorted prior to ipilimumab) loaded with various bacterial strains (as indicated, bacteria neutralized with antibiotics before coculture with T cells) in duplicate wells. IFN γ (**A**) and IL-10 (**B**) were monitored in the supernatants by commercial ELISA or by luminex Magpix technology at 48 hrs. No cytokine release was observed in the absence of bacteria or with loaded monocytes in the absence of T cells. Each dot represents cytokine secretion of an individual patient. **C** Id as in A in paired analyses. Compared with healthy volunteers (HV) (A, left panel), cancer patients exhibited a baseline decreased commensal-specific Th1 immunity (A, middle panel) that, at least in some cases, could be restored by CTLA4 blockade (A, right panel) with a concomitant drop in IL-10 release (B). Ipilimumab significantly increased IFN γ secretion by T cells responding to *Bf* and *Bt* (but not irrelevant bacteria, Fig. 3D) in MM but not in NSCLC patients (C). **D.** depicts the IFN γ /IL-10 ratio in MM and NSCLC (lung) patients for pre- and post- ipilimumab for TCR, *B.*

fragilis and *B. thetaiotaomicron* stimulation. Memory T cells from NSCLC patients tend to respond to *Bc* by augmenting their IFN γ /IL-10 cytokine release ratio (Fig. 3E, and D).

Supplementary Figure 12. Adoptive T cell transfer of T cells restimulated with *Bacteroides* species into ACS-treated tumor bearers injected with 9D9 Ab. T cells harvested from spleens of mice exposed to 9D9Ab and restimulated with *Bf* (as stated in Fig. 2C. at 1:10 ratio) pulsed onto BM-DC or BM-DC alone (CD4⁺ NT) were infused iv in day 6 MCA205–tumor bearing antibiotics (ACS)-treated mice. A representative experiment containing 5-6 mice/group is shown. Longitudinal analysis did not indicate significant differences between the three groups ($p < 0.1970$ between the CD4⁺ NT group and the CD4⁺ *B. fragilis* group). However, using the last recorded measurement (D19), the CD4⁺ NT group was found to be 1.44 fold higher than the CD4⁺ *B. fragilis* group ($p < 0.07$) and the CD4 NaCl group was found to be 1.36 fold higher than the CD4⁺ *B. fragilis* group ($p < 0.18$).

Supplementary Figure 13. *Bf*-induced IL-12 production by DC is mandatory for the antitumor effects of CTLA4 blockade. **A.** Changes in DC subsets in the colonic lamina propria (LP) during CTLA4 blockade. Enumeration of percentages of pDC and CD11b⁺ DC gated on CD45⁺CD11c⁺I-A^b cells by flow cytometry of colonic LP harvested after 2 injections of 9D9 (versus Iso Ctrl) Ab in 6 naïve animals in a graph indicating the mean percentages \pm SEM. **B.** Maturation of LP DC. Mean expressions \pm SEM of CD86 in DC subsets of colon or mesenteric LN LP are depicted for 6 animals per group. A brisk loss of plasmacytoid DC in the colon accompanied by their local maturation with a progressive accumulation of LP-CD11b⁺DC and a concomitant maturation in mesenteric lymph nodes of CD103⁺ DCs and CD103⁺CD11b⁺ DCs was observed. **C.** Role of IL-12 in the antitumor effects of CTLA4 blockade. IL-12p70 production by CD11b⁺ DC loaded with *B. fragilis* or PS enriched fractions of *B. fragilis* and other isolates (as listed) as determined in commercial ELISA at 24 hrs (C) in triplicate wells in 1-4 experiments (each dot representing one well). **D.** Neutralisation of IL-12 blunts the antitumor effects of 9D9 Ab. Neutralizing anti-IL-12p40 Ab (or irrelevant Iso Ctrl Ab) administered in experimental settings described in M&M, and tumor sizes overtime in SPF conditions- reared mice (**D**). The anti-CTLA4 Ab-mediated antitumor effects were significantly reduced by a neutralizing anti-IL-12p40 Ab. **E.F.** Depict a similar experiment where GF mice monoassociated or not with *B. fragilis* were treated or not with anti-IL-12p40 Ab. Tumor sizes at day 8 are shown (**E**). **F** shows CD80 MFI levels on tumor DCs taken at day 8 post the start of anti-IL12p40 Ab treatment. Neutralizing IL-12 in GF animals mono-associated with *Bf* suppressed the antitumor effects of CTLA4 blockade and CD80 upregulation in intratumoral DC. **G.** Intravenous adoptive transfer of 1×10^6 BM-DC pulsed with PS enriched fractions of *B. fragilis* (or polysaccharide-enriched capsule of *B. distasonis*), I-A^b-restricted KD peptidomimetic of zwitterionic motifs (12), or unpulsed (mock) controls, in tumor bearers treated with antibiotics and then anti-CTLA4 Ab. Loading of CD11b⁺ DC with purified polysaccharides from *Bf* capsules (PS) (composition defined by capillary electrophoresis presented in Supplemental Fig. 14A) followed by iv administration into ACS-treated mice rendered CTLA4 blockade more effective in ACS-treated mice when DC were pulsed with *Bf* antigens (PS), but not when they were pulsed with *B. distasonis* capsules (composition detailed in Supplemental Fig. 14A) or the KD peptides. One representative experiment out of two yielding similar results of tumor growth kinetics for 5 mice/group is depicted. Anova statistical analyses: * $p < 0.05$, ** $p < 0.01$, *** $p < 0.001$, ns: not significant.

Supplementary Figure 14. Monosaccharide analysis of the capsular polysaccharide-enriched fractions from *B. fragilis* and *B. distasonis* and the antitumor effects mediated by oral feeding with capsular polysaccharide enriched fractions of *Bacteroides* spp. **A.** Monosaccharides from *B. fragilis* and *B. distasonis* capsular polysaccharide-enriched fractions were analysed as described in M&M by capillary electrophoresis monitored by laser-induced fluorescence (CE-LIF). The *B. distasonis* capsular polysaccharide-enriched fraction was devoid of galacturonic acid and contained a much lower amount of fucose (lower panel, red arrows; this was also confirmed by GC analysis (not shown)). **B.** C57BL/6 ACS-treated mice were orally administered the enriched capsular polysaccharide fractions of *B. distasonis*, or *B. fragilis*, at doses of 0.5, 5, or 50 µg per mouse, six days after treatment with anti-CTLA4 mAb. Control mice received anti-CTLA4 mAb alone, with or without prior ACS administration, or isotype control mAb without ACS. Tumor sizes from mice 6 days following mAb with PS doses for each *Bacteroides* spp. combined. The numbers of protected mice, as determined for the anti-CTLA4 Ab-treated control group, are displayed. Oral feeding of ACS-treated mice with *Bf* PS (but not *B. distasonis* capsules) was sufficient to increase the efficacy of CTLA4 blockade in half of the animals, suggesting that live *Bf* is more efficient than its inert antigens in stimulating an efficient anticancer immune response.

Supplementary Figure 15. TLR2 and TLR4 were partially involved in anti-CTLA4-mediated tumor control. C57BL/6 WT, *Tlr2*^{-/-}, or *Tlr4*^{-/-} mice bearing MCA205 tumors (**A**), or BALB/c WT and *Tlr4*^{-/-} mice bearing CT26 tumors (**B**), were administered anti-CTLA4 or isotype control Ab as detailed before. Tumor growth and tumor-free animals were recorded as shown. The Kaplan-Meier survival curves for different treatment regimens are depicted (right panel) for one representative experiment containing 5-6 mice/group (log-rank analysis $p < 0.05$). In *Tlr2*^{-/-} and *Tlr4*^{-/-} hosts, the anti-CTLA4 partially lost its efficacy. **C** depicts MCA205 tumor growth in C57BL/6 mice administered the TLR2 and TLR4 ligands lipoteichoic acid and *E. coli* lipopolysaccharide respectively, as detailed in the M&M. Oral administration of such TLR agonists failed to restore the anti-CTLA4-induced antitumor effects lost in ACS-treated mice. Data shown are from one of two independently performed experiments ($n = 6$).

Supplementary Figure 16. CTLA-4 expression on lymphocyte subsets of the intestines at baseline and post-CTLA4 blockade. Intestinal lymphocytes were isolated from the small intestines and colons. CTLA-4 expression was determined (surface and intracellular staining combined) (A, at baseline) as well as surface expression without permeabilization (B, after anti-CTLA4 Ab) in the indicated lymphocytic populations. Representative overlay are shown for one experiment. C. ICOS expression on effector CD4⁺ T cells harvested from the lamina propria of the colon 2 days after the third administration of 9D9 or Iso Ctrl. * $p < 0.05$, ns = not significant by unpaired two-tailed *t*-test.

Supplementary Figure 17. Co-blockade of IL-10 and CTLA4 provokes colitis and tumor escape. Small intestines and colons from *Il-10*^{-/-} or WT C57BL/6 mice were taken and processed for histopathological scoring (as detailed in the Materials & Methods) from MCA205 tumor-bearing mice 8 days after beginning αCTLA4 (or isotype control) mAb therapy as detailed

before. **A** shows a representative picture of colon sections from each group. The level of colitis was scored from at least 8 distinct regions from each mouse (**B**). **C**. Tumor growth kinetics with or without α CTLA4 Ab in various genetic backgrounds in BALB/c mice. BALB/c WT, $Il10^{-/-}$ and $Il10^{-/-}$ x $Nod2^{-/-}$ mice bearing CT26 tumors were administered anti-CTLA4 or isotype control as before, and tumor growth kinetics were recorded and depicted in **C**. Mice deficient in IL-10 (but not NOD2, not shown) manifested exacerbated histopathological signs of intestinal toxicity upon anti-CTLA4 administration, although they failed to control tumor growth in response to CTLA4 blockade, suggesting that the antitumor efficacy of CTLA4 blockade is not related to colitis severity. Scale bar in **A** is 100 μ m. *** $p < 0.001$ by proportional odds logistic regression in **B**. Data shown in **C** depict the means \pm SEM ($n = 5-8$), *** $p < 0.001$, ns: not significant.

Supplementary Figure 18. Co-blockade of ICOS and CTLA4 induced overt Th1 responses and animal death. **A-C.** *Th1, pTH17 and Tc1 systemic immunity during the ICOS/CTLA4 co-blockade.* MCA205 tumor-bearing C57BL/6 mice were administered anti-ICOS or isotype control mAbs on commencement of α CTLA4 (or isotype control) mAb therapy. At day 10 post mAb treatments, splenocytes were isolated and IFN- γ ⁺ (**A**) and IFN- γ ⁺IL-17⁺ (**B**) CD4⁺ T cells and CXCR3⁺ CD8⁺ T cells (**C**) were determined by flow cytometry following 4h stimulation with PMA and ionomycin. **D.** *Lethal effects of the ICOS/CTLA4 coblockade.* Figure shows the percentage death per group of mice from three independent experiments. Data shown depict the mean \pm SEM ($n = 5$). * $p < 0.05$ by one-way ANOVA with Bonferroni's multiple comparison test. Hence, in normal C57BL/6 mice, simultaneous blockade of CTLA4 and ICOS induced a strong increase in splenic TH1, Tc1 and pathogenic TH17 cells, eventually causing death of 20% of the animals. Hence, monotherapy with CTLA4-blocking Ab does not affect the major pillars of gut tolerance (IL-10, NOD2, or ICOS), and colitis is not required for the improvement of anticancer immunosurveillance elicited by CTLA4 blockade (Suppl. Fig. 17, 18).

Supplementary Figure 19. No role for neutrophils in efficacy or toxicity of anti-CTLA4 Ab.

A. *Microbiota-dependent neutrophil accumulation in tumors.* Tumoral neutrophils (Ly6G⁺CD45⁺) were determined by flow cytometry in SPF and ATBx-treated MCA205-bearing C57BL/6 mice at 8 days post anti-CTLA4 (or isotype control) mAb therapy (**A**). Each dot represents one mouse tumor. **B-D.** *Neutrophil depletion does not prevent antitumor efficacy of CTLA4 blockade.* In an additional experiment, mice were administered anti-Ly6G (1A8 Ab or isotype control) mAb every other day on commencement of α CTLA4 (or isotype control) mAb therapy, and neutrophil depletion was confirmed for each mouse from blood sampling 7 days later (post- 4 anti-Ly6G injections) by flow cytometry as depicted by the representative dot plots shown in **B** Tumor growth for control or neutrophil-depleted mice is shown in **C** (left and right panel) for a representative experiment out of two yielding similar results. **D.** *Neutrophil depletion does not prevent gut toxicity.* Colons harvested from these mice, 15 days post the start of mAb therapy were sectioned for colitis scoring as detailed in Materials & Methods. Neutralization of nitric oxide using the iNOS inhibitor L-NMMA was performed at the onset of CTLA4 blockade and did not alter the antitumor effects (**E**). Tumor sizes at day 9 post 9D9 or Iso Ctrl Ab-treatment are depicted (**E**). Each dot represents one tumor and graphs depict 2 experiments of 5 mice/group. * $p < 0.05$, ns = not significant, by one-way ANOVA with Bonferroni's multiple comparison test in **A** and **E**. ** $p < 0.01$, ns = not significant, by proportional odds logistic regression in **D**. * $p < 0.05$, ns = not significant, by unpaired two-tailed *t*-test (**C**). Hence, the depletion of neutrophils which were increased in tumors post- CTLA4

blockade in a microbiota-dependent manner, or the neutralization of their main metabolite, nitric oxide, failed to affect gut toxicity or treatment efficacy.

Supplementary Figure 20. Clustering of patients before and during ipilimumab therapy. A.

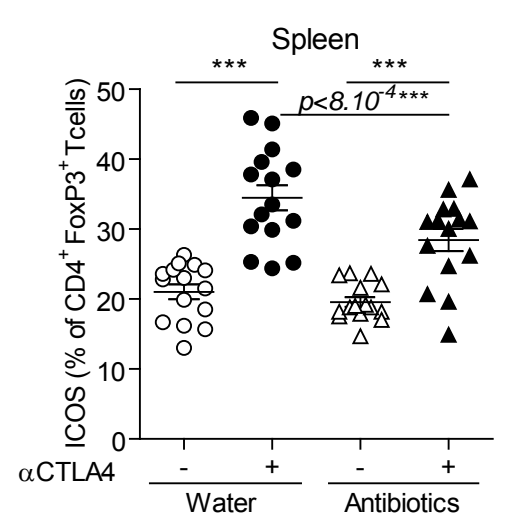
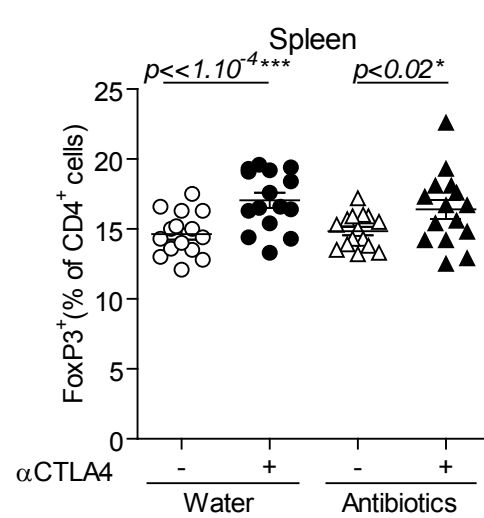
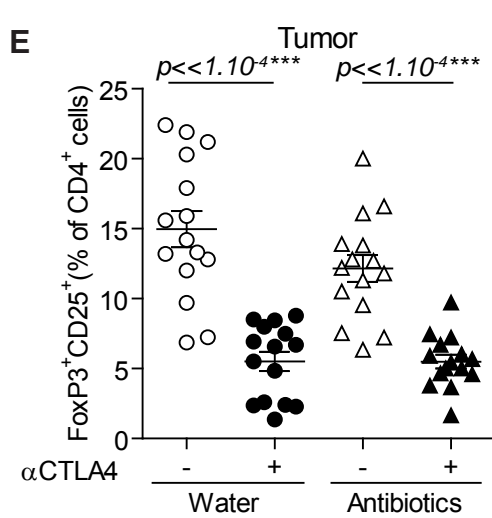
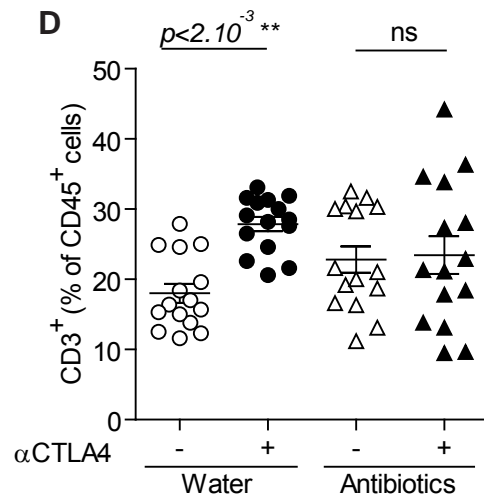
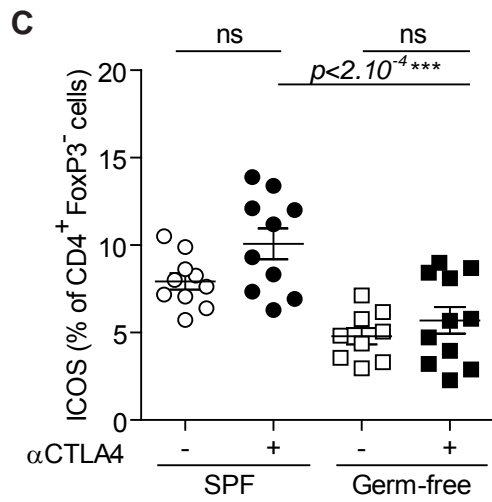
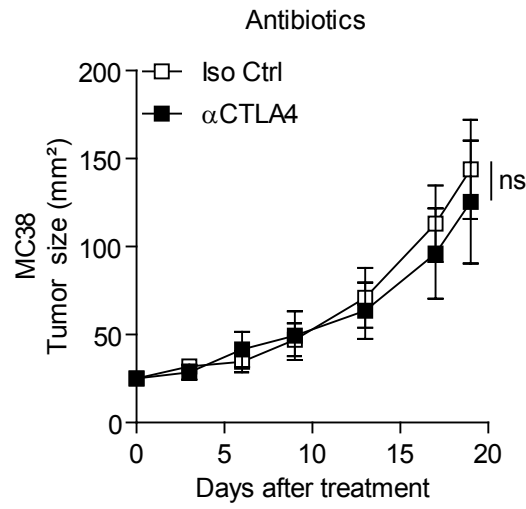
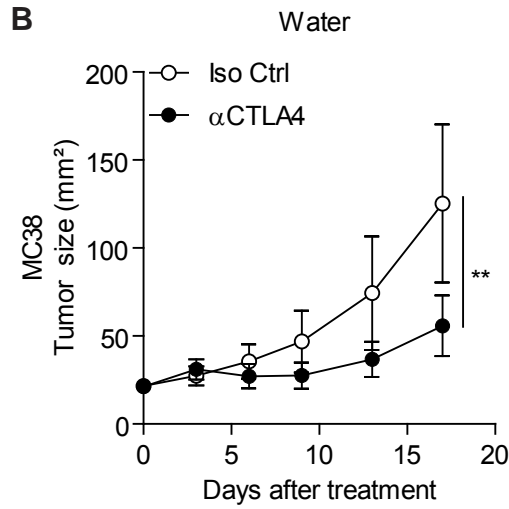
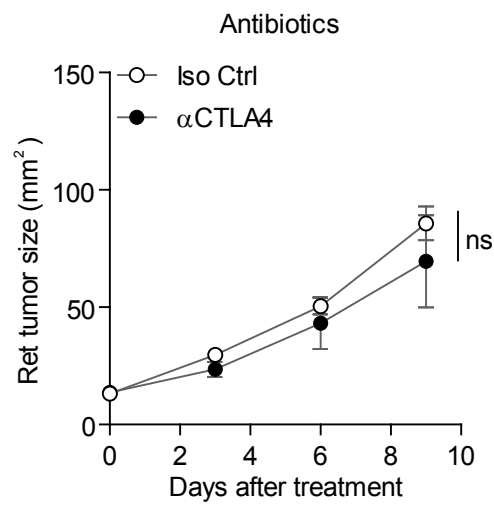
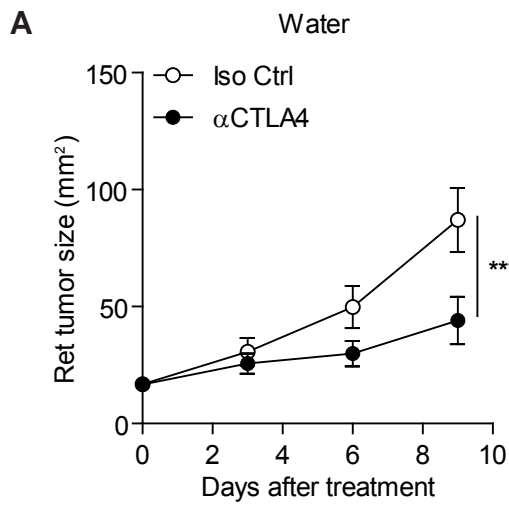
Composition of the gut microbiome before and after ipilimumab treatment. A clustering algorithm based on genus composition was applied to cluster patients into one of three enterotypes as described in Fig. 4A-B. Follow up detailed chart of the clustering for each patient over time. * indicates the feces samples utilized for the FMT described in Fig. 4C-E. **B.** Quantification of bacteria in mouse feces after α CTLA4 treatment. QPCR analyses on feces DNA using specific probes targeting *Bacteroides/Prevotella* group and *Bacteroides* species *B. fragilis* and *B. thetaiotaomicron* in mice feces at day 12 after α CTLA4 treatment (n=15-19 for each cluster) compared with isotype control-treated mice (n=5). Each dot represents one mouse. Mann-Whitney t test : **p<0.01. **C.** Correlation between tumor size and *B. thetaiotaomicron*, *B. uniformis* and *B. distasonis* abundance. Tumor sizes at day 12 after CTLA4 treatment and *Bacteroides* species abundance (normalized to total bacteria) at the same day were analyzed for FMT recipient mice from clusters C. Spearman r and p values are shown in each graph. No correlation was achieved for cluster B. In cluster A, no detectable amount of *Bacteroides* spp. could be detected (Fig. 3B, right panel). These microbial shifts observed in MM allow to postulate that the therapeutic antibody (ipilimumab) is capable, in some patients, to influence the microbial composition in the favorable direction (driving patients' stools from a B to a C enterotype, Fig. 4) at some point in the course of the therapy. In a non paired analysis comparing the distributions of the three enterotypes before (in 19 stools at T0) versus after ipilimumab (in 18 stools at T>0 (at any time point after one injection), we observed 11B/19 (58%) and 5C/19 (26%) before versus 39% and 39% respectively at any time point after therapy, suggesting a conversion of some patients' feces towards a more immunogenic enterotype. In a paired analysis of feces performed in 12 cases, the calculations indicated that out of the 7 stools of a B pattern, only 2 (29%) turned into the C favorable enterotype. We postulate that ipilimumab could modify the pattern of enterotypes and after 1 or 2 injections of ipilimumab, about one third of individuals may fall into the favorable cluster C. Cluster A (a rare enterotype in MM patients) stools appeared to also condition or predict to some extent the antitumor effects mediated by ipilimumab, suggesting that some other family members of the *Bacteroidales* genus (i.e *Prevotella*) could also ignite antitumor immunity..

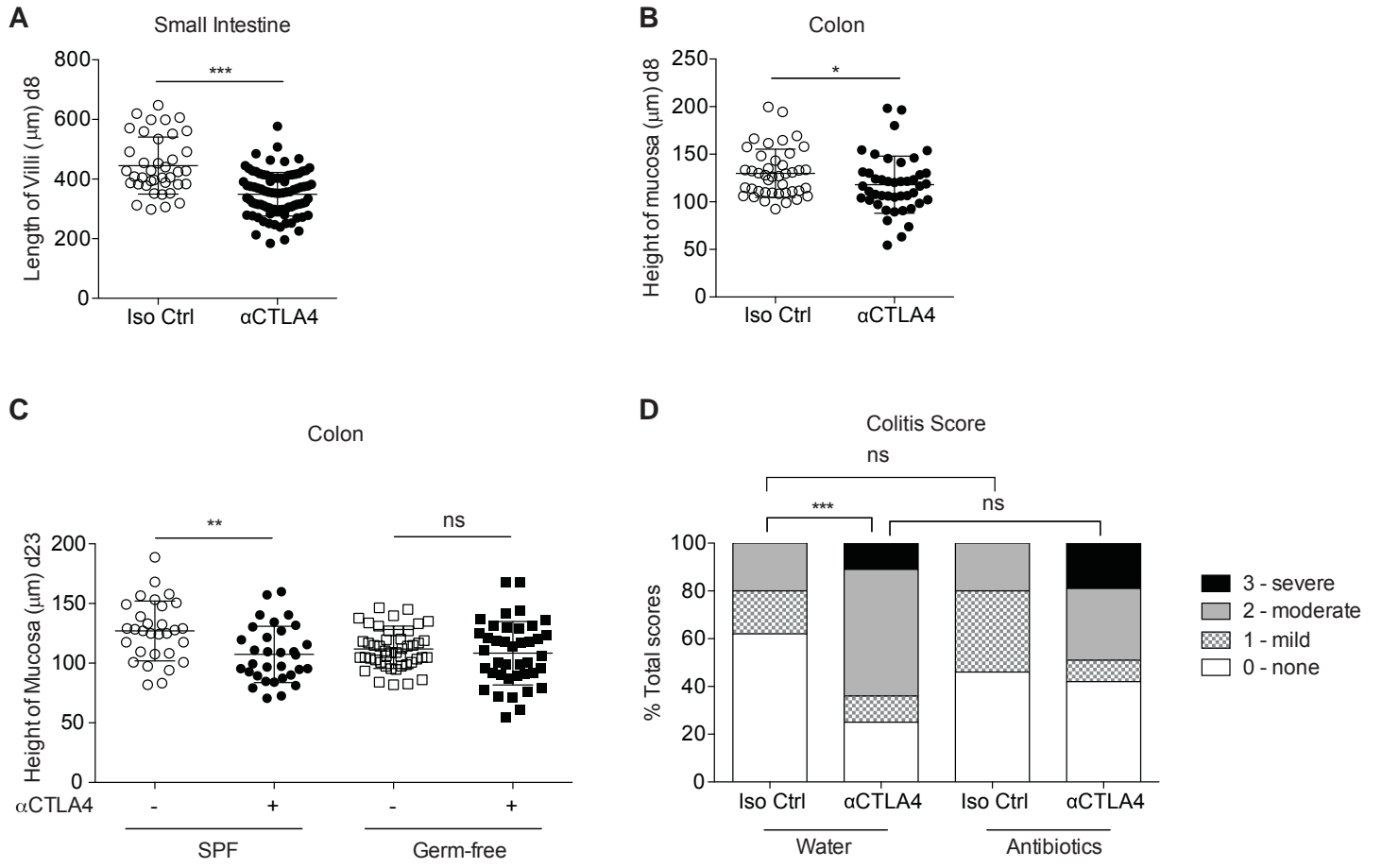
Supplementary Figure 21. Vancomycin augments the tumoricidal effects of CTLA4 blockade.

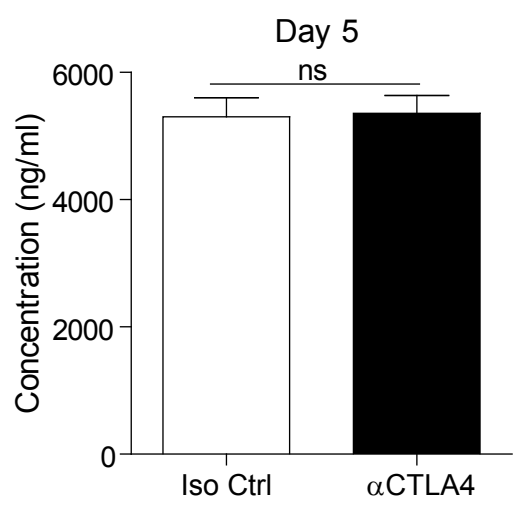
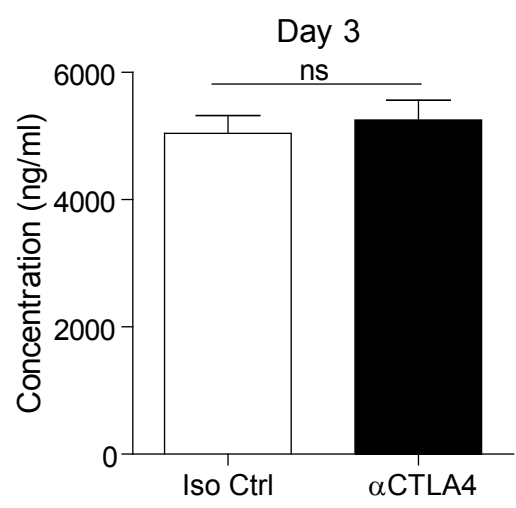
Vancomycin prevented the loss of *Bacteroidales* and *Burkholderiales* orders induced by anti-CTLA4 Ab (A). Sequencing of 16S rRNA gene amplicons of feces of tumor bearers before and 48 hrs after one ip administration of 9D9 or isotype control Ab in the setting of a vancomycin conditioning (details in Suppl. Table 1). Means \pm SEM of relative values for each order for 5 mice/group are shown. The effects of vancomycin (vanco)-conditioning on mice inoculated at day 14 with MCA205 and treated at day 2 post-tumor inoculation with 9D9 (or iso Ctrl) Ab are shown. Tumor growth curves are depicted from 2 experiments (B. left panel) or at day 15 post-9D9 or Iso Ctrl Ab-treatment (B. right panel). **C.** Histopathological score of colonic mucosae in vancomycin-treated tumor bearers receiving anti-CTLA4, established on H&E stained colons as described in M&M at day 20 in 5 animals/group for at least 6 independent

areas (right panel). Anova statistical analyses, histopathological scoring by proportional odds logistic regression, * $p < 0.05$, ** $p < 0.01$, *** $p < 0.001$, ns: not significant.

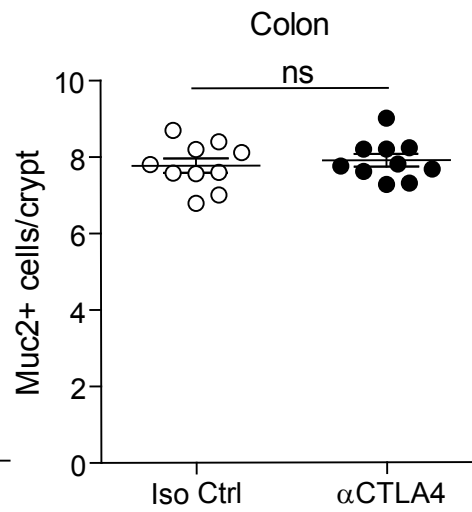
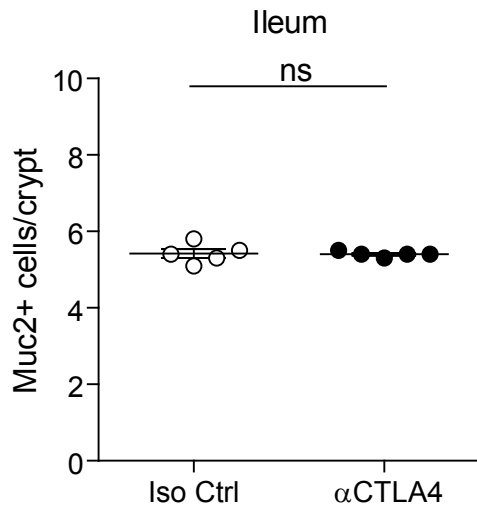
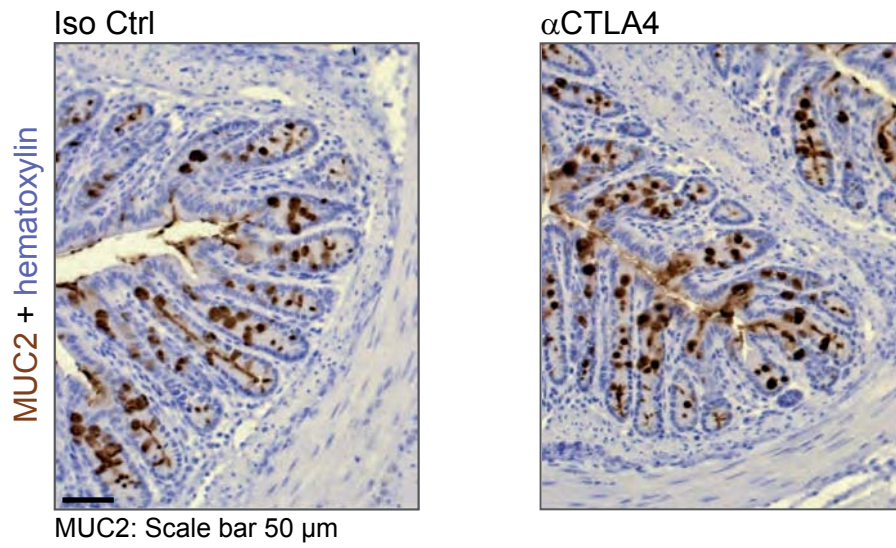
Supplementary Figure 22. *Bf* induced Treg activation in GF mice with no dramatic effects of CTLA4 blockade. Tumor draining lymph nodes (black dots) and contralateral lymph nodes (grey triangles) were collected from SPF, GF, or GF mice monoassociated with *B. fragilis* treated with 9D9 or isotype control Abs at d20 post-treatment. Ki67 (A) and ICOS (B) expression on Tregs were monitored by flow cytometry. * $p < 0.05$, ns = not significant, by Student t' test. Hence, *Bf* could not only elicit IL-12-dependent Th1 immune responses in cancer bearing hosts (Fig. 3), but also upregulated ICOS expression and proliferation of splenic Tregs during anti-CTLA4 Ab treatment of *Bf* mono-associated GF animals. The division of labor of pDC versus CD11b⁺ DC might explain this dual phenomena (7).



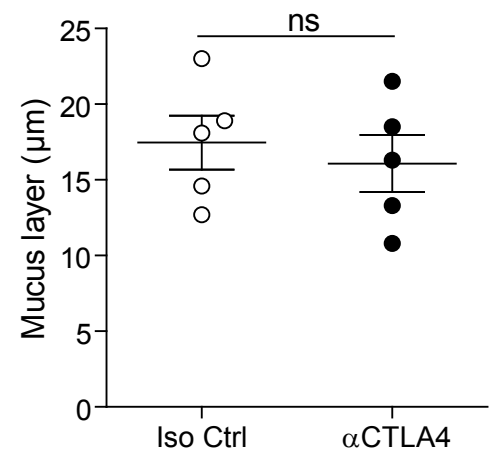


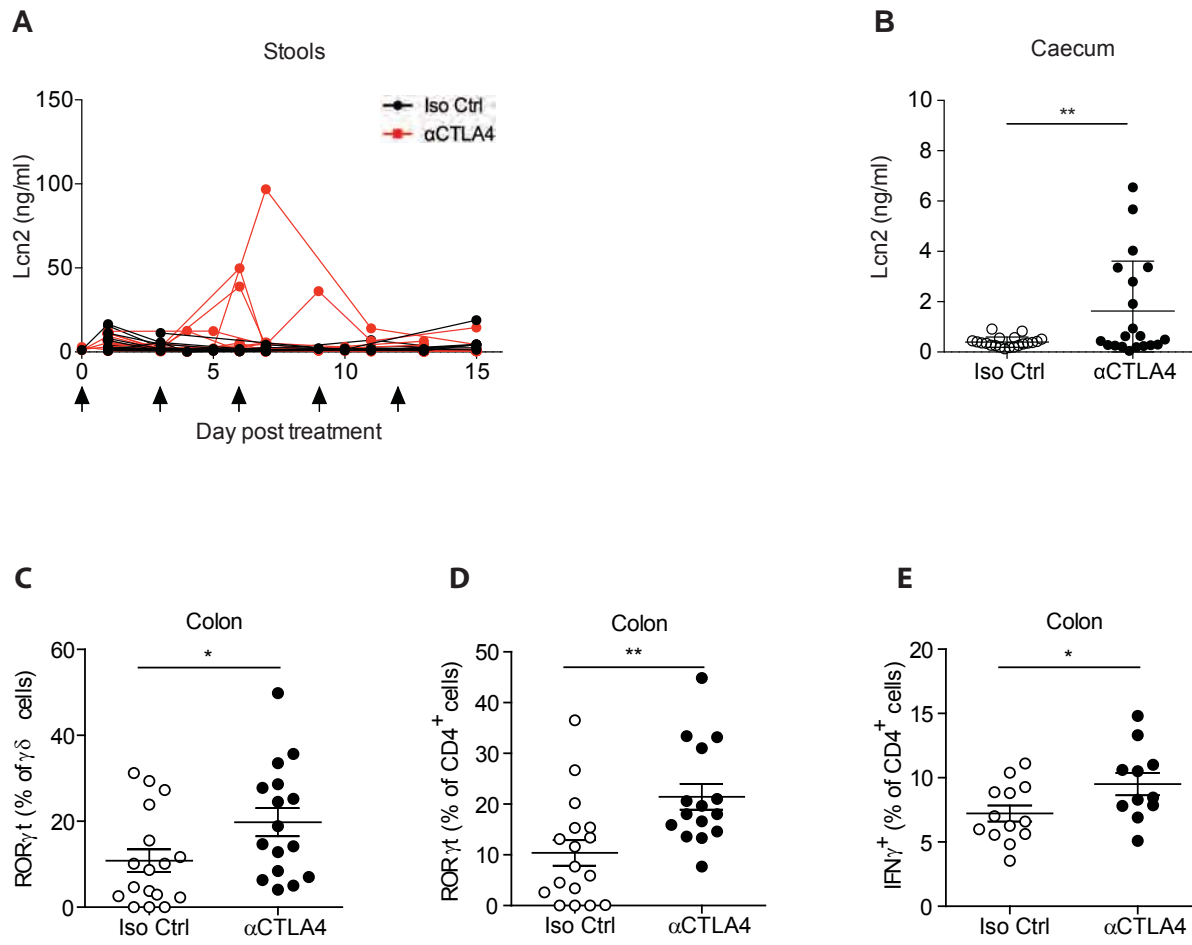


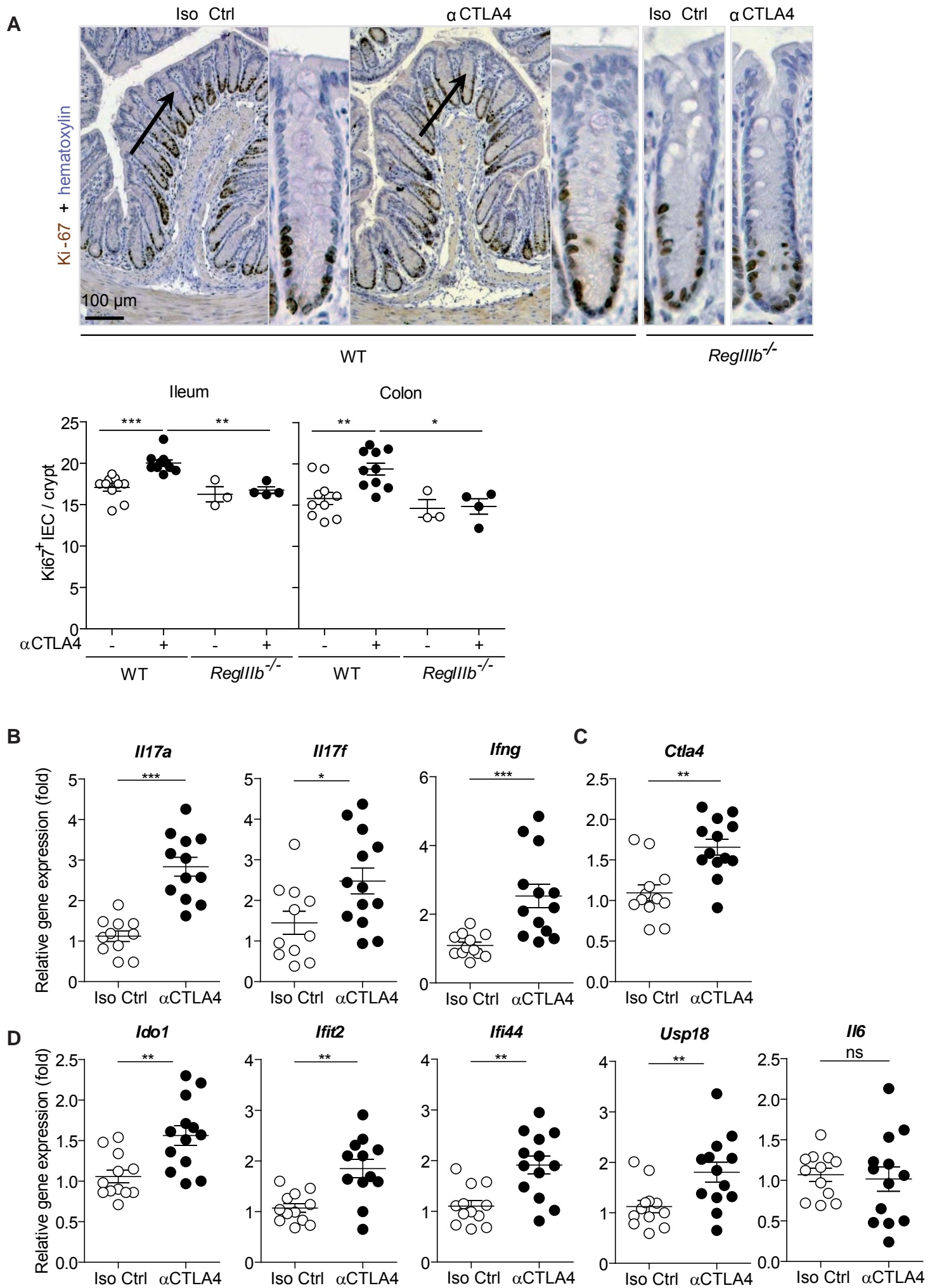
A

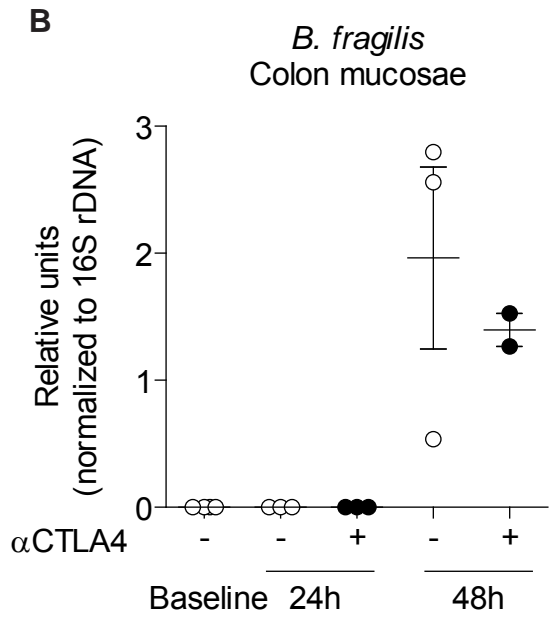
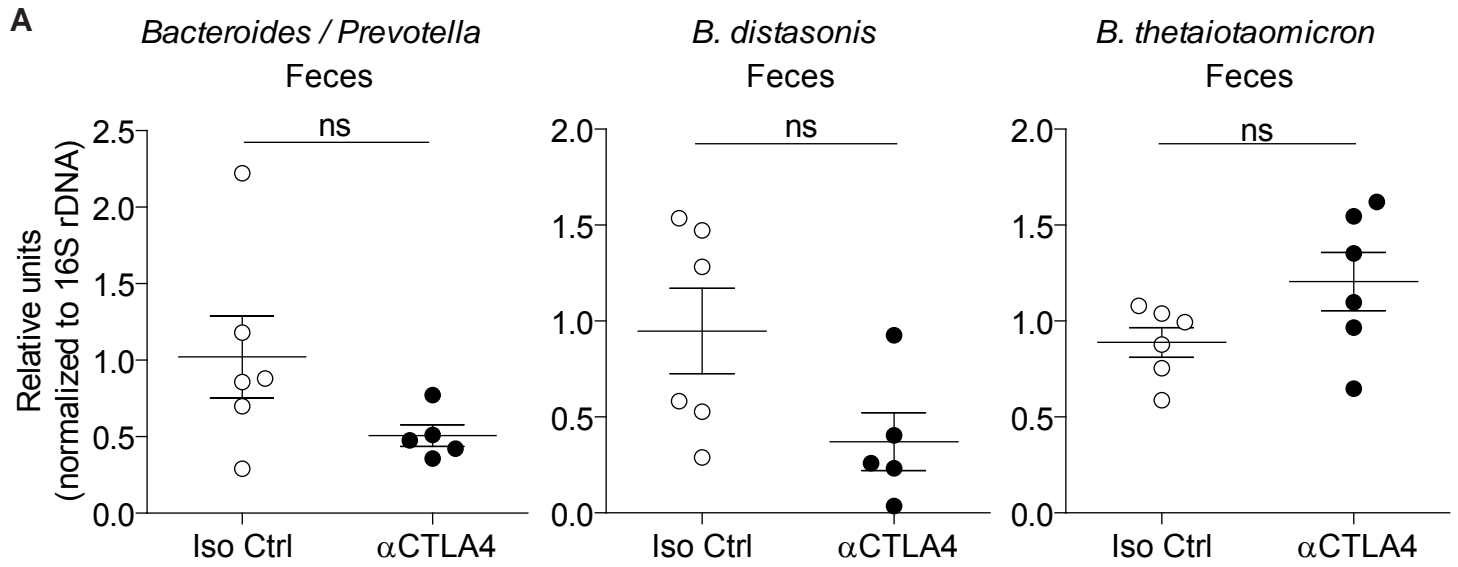


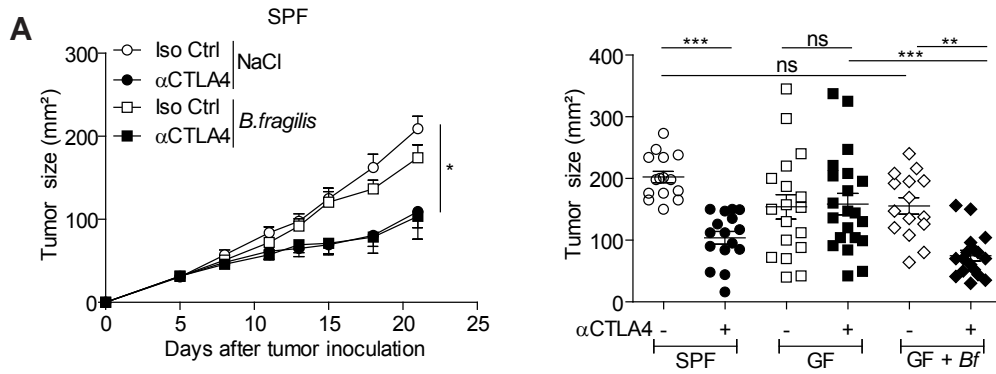
B



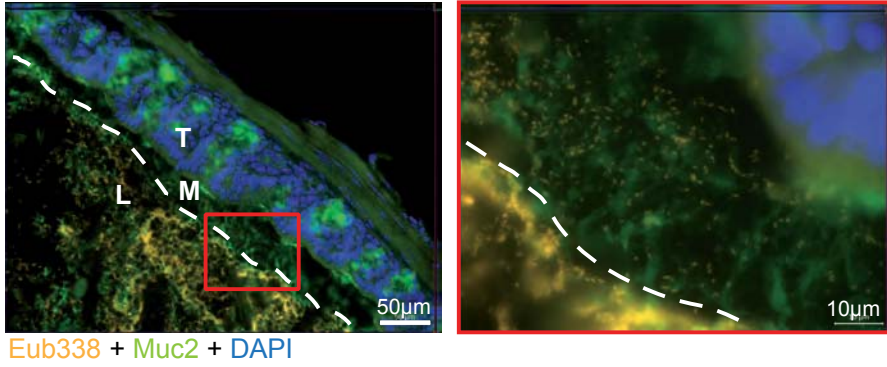




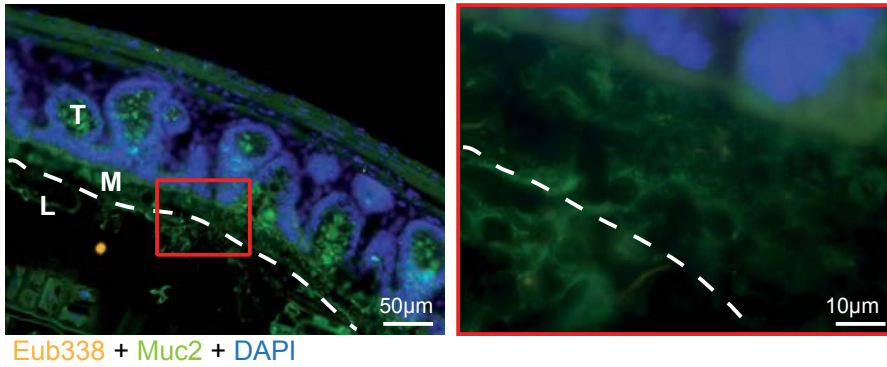




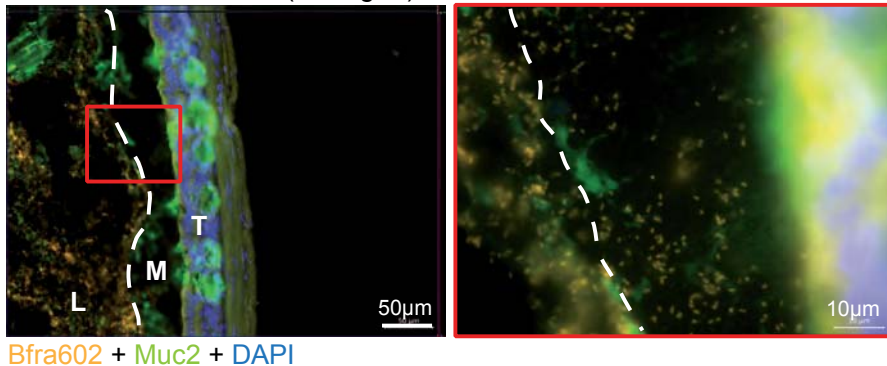
B Mono-associated mice (*B. fragilis*)



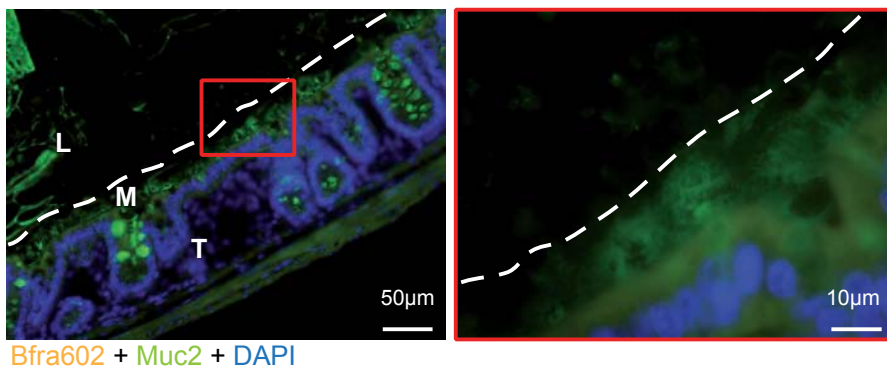
Germ-free control

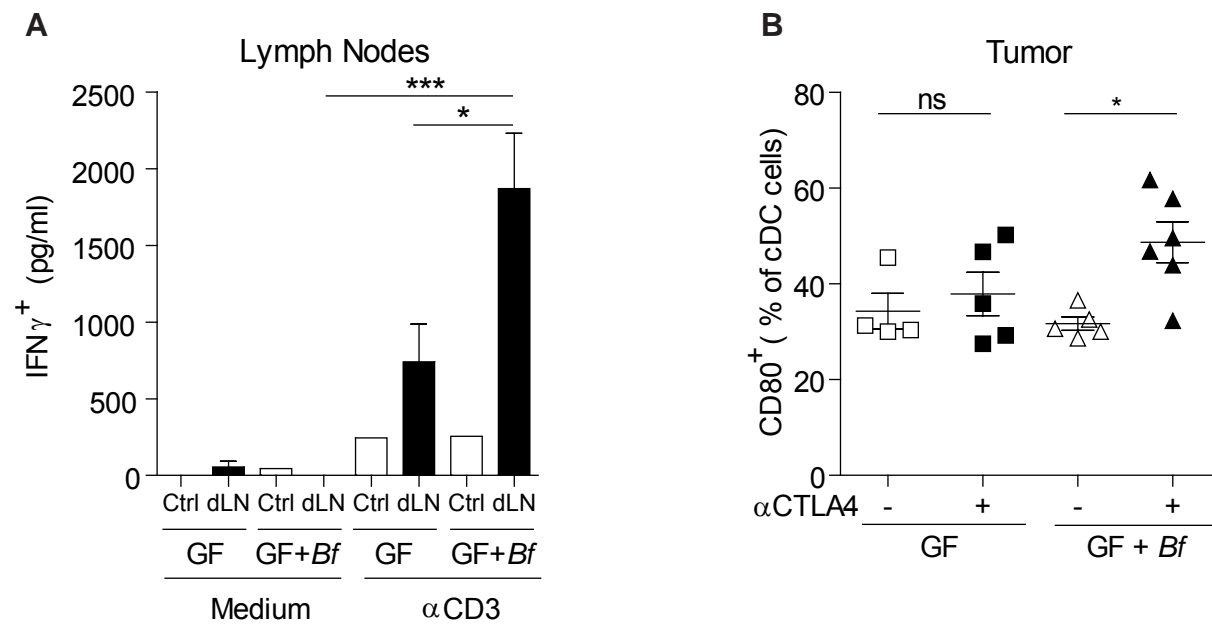


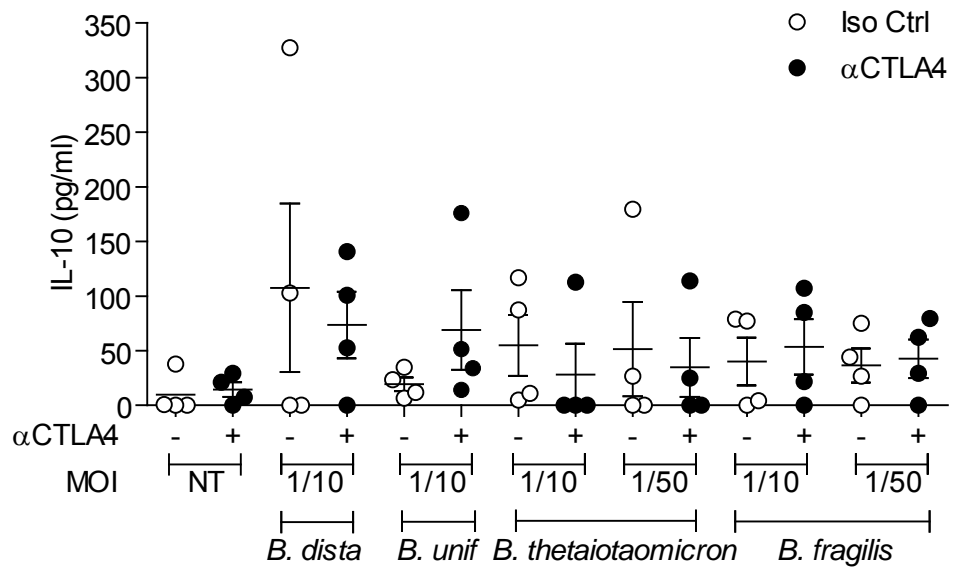
C Mono-associated mice (*B. fragilis*)

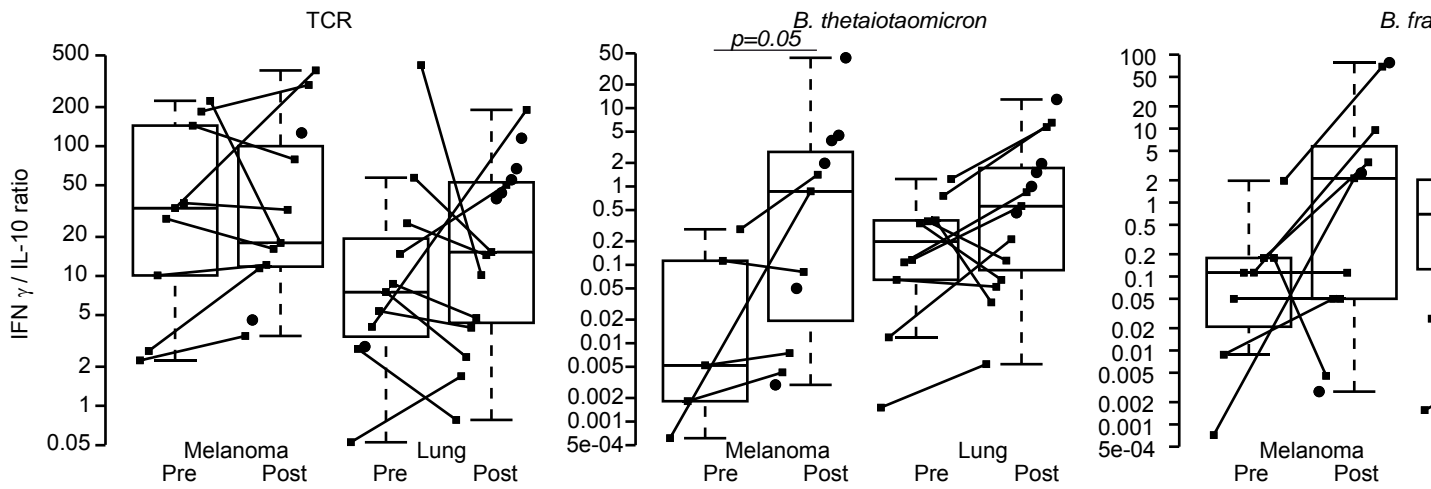
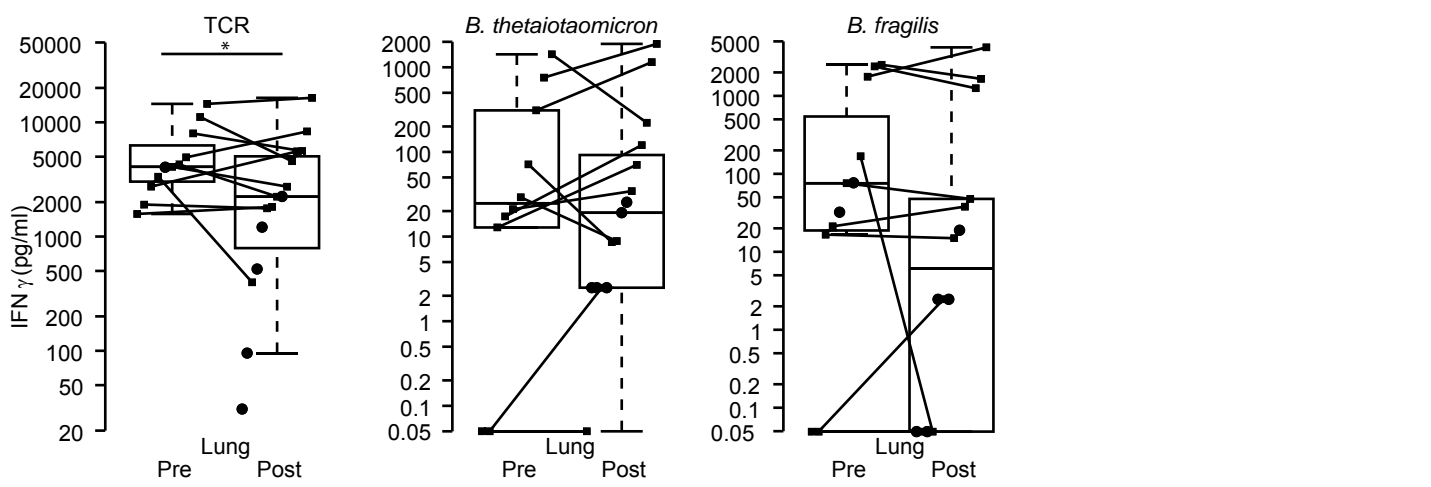
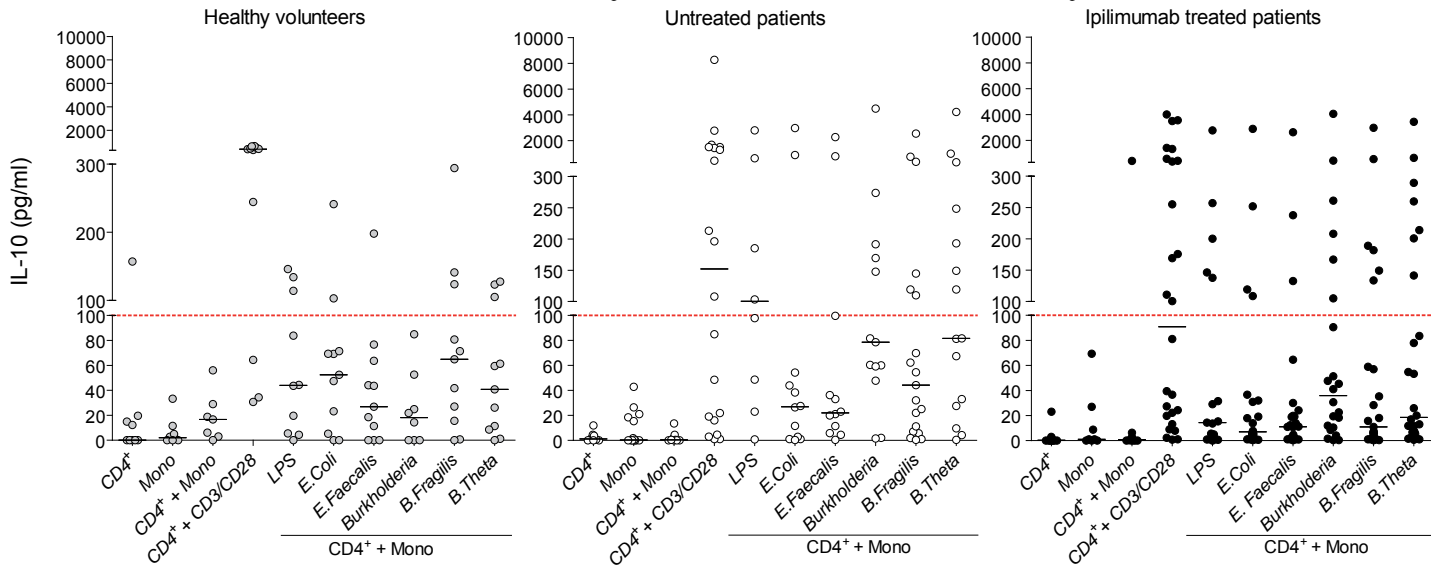
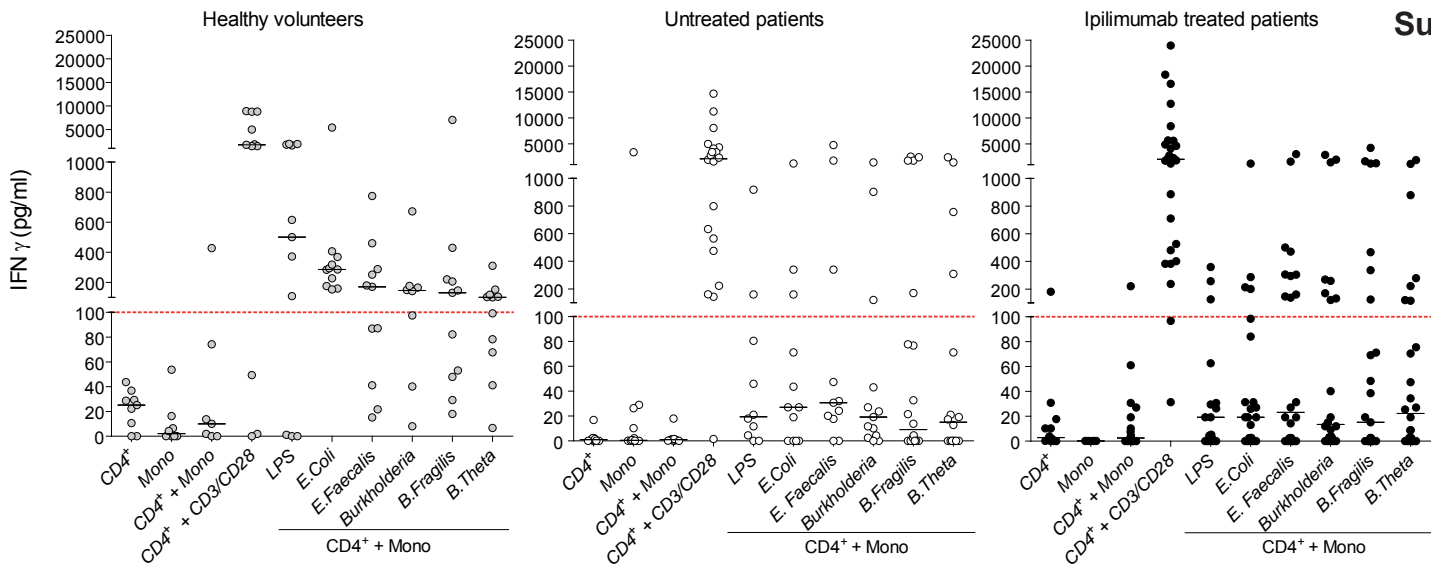


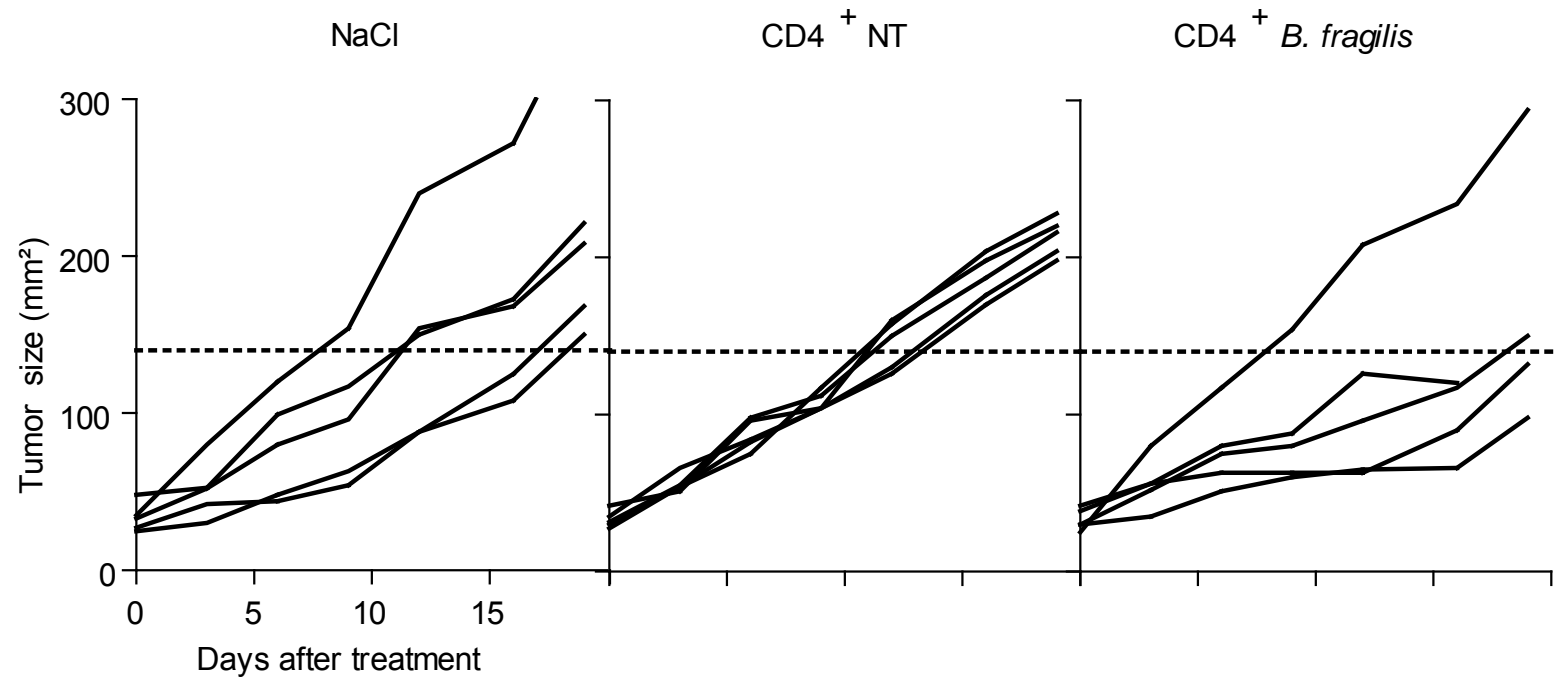
Germ-free control

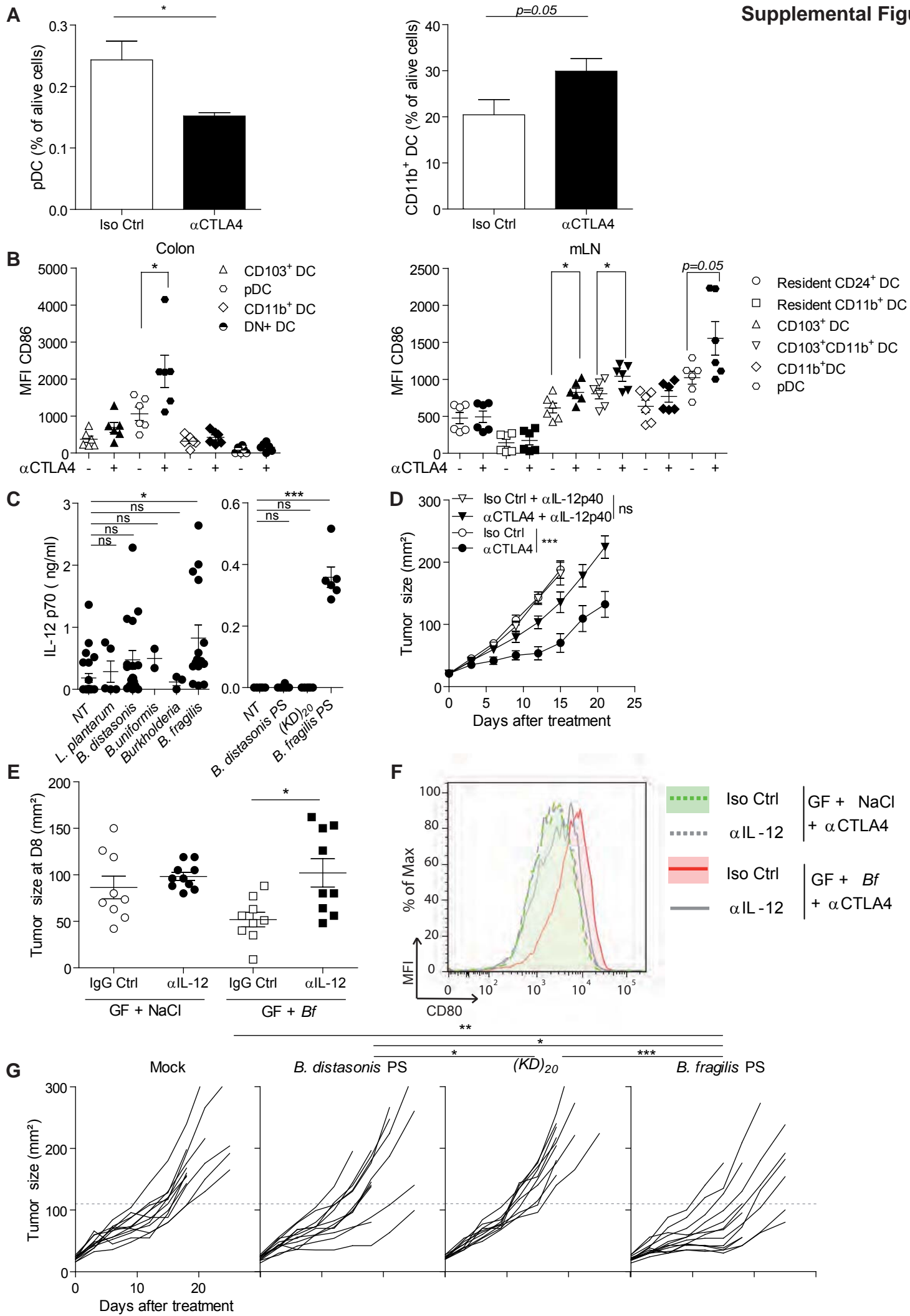




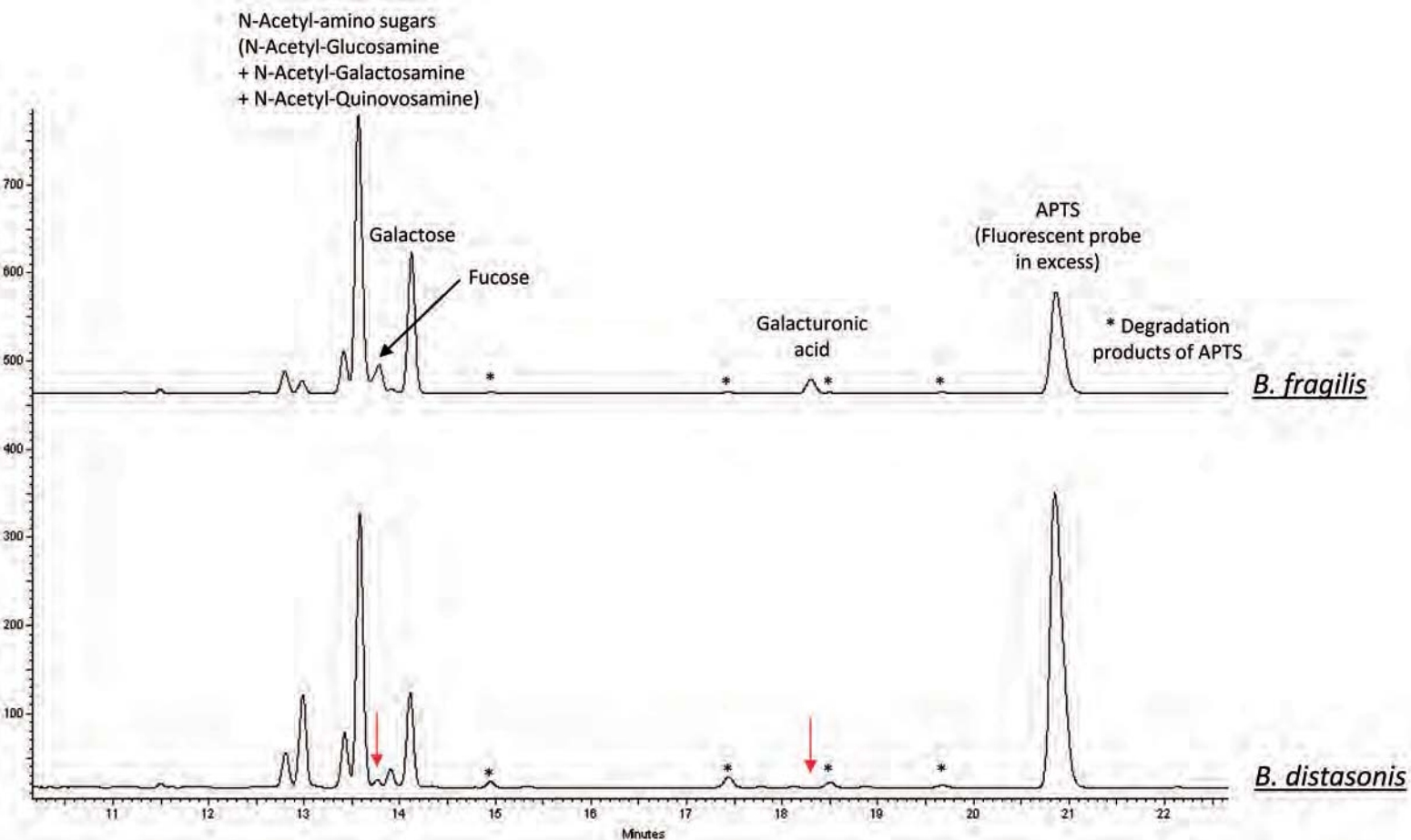




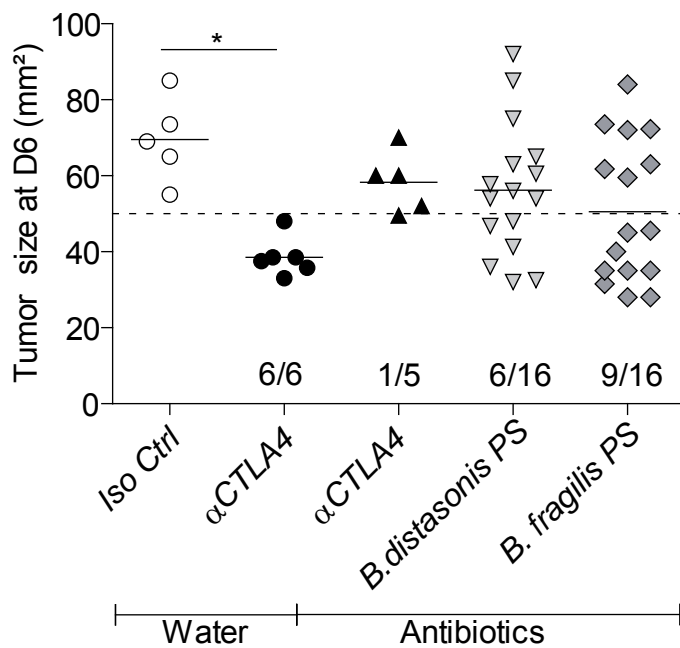


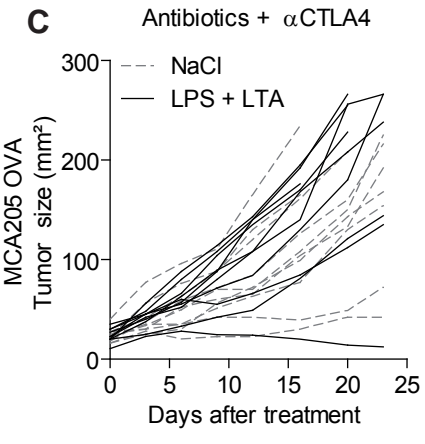
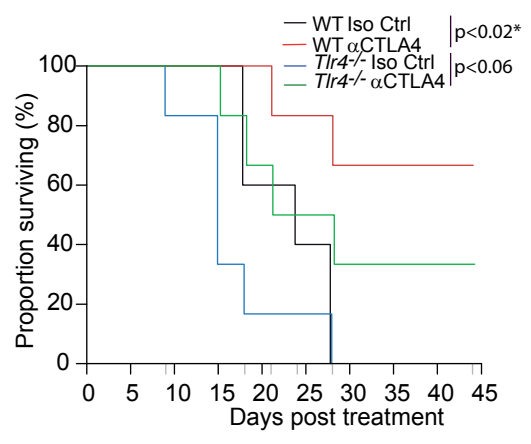
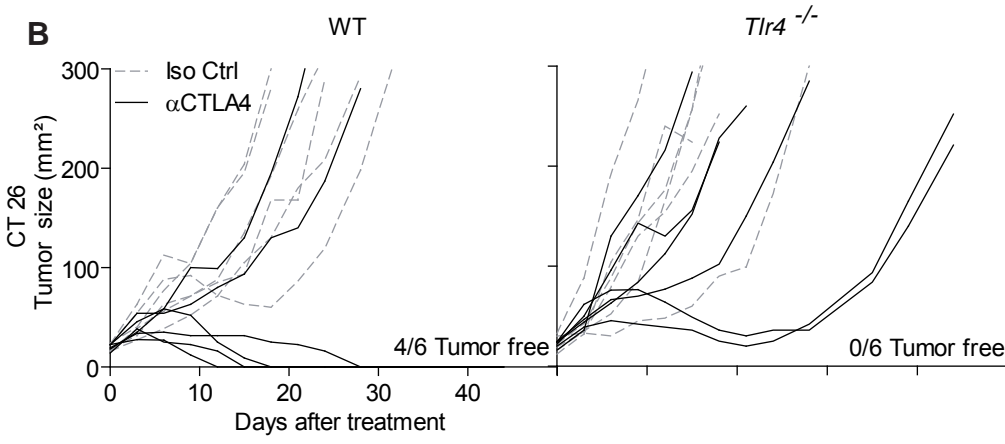
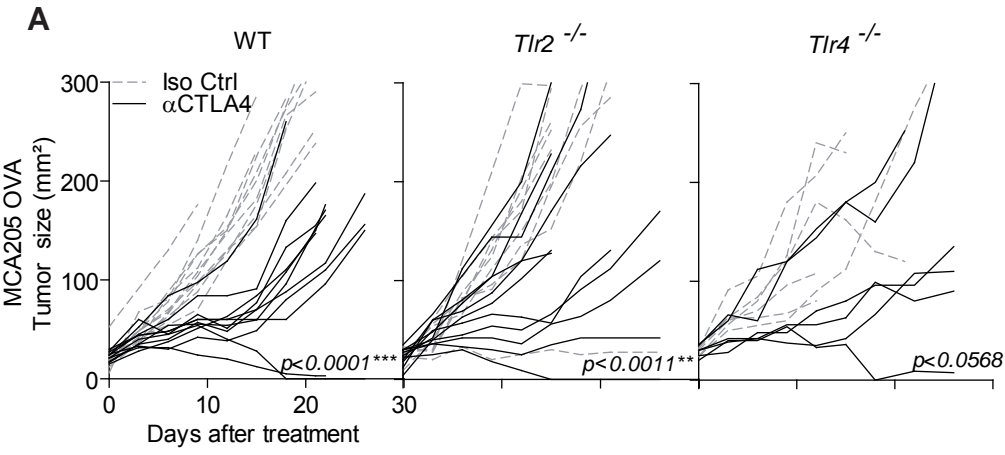


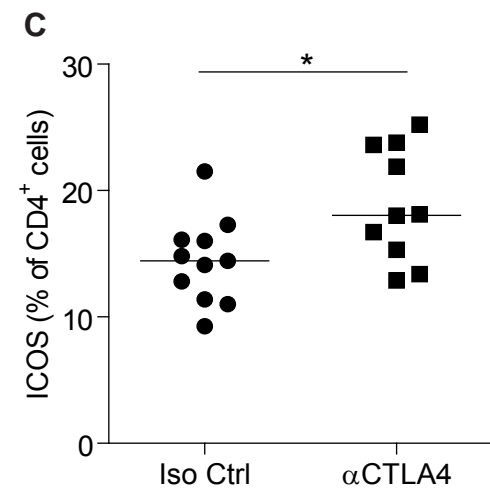
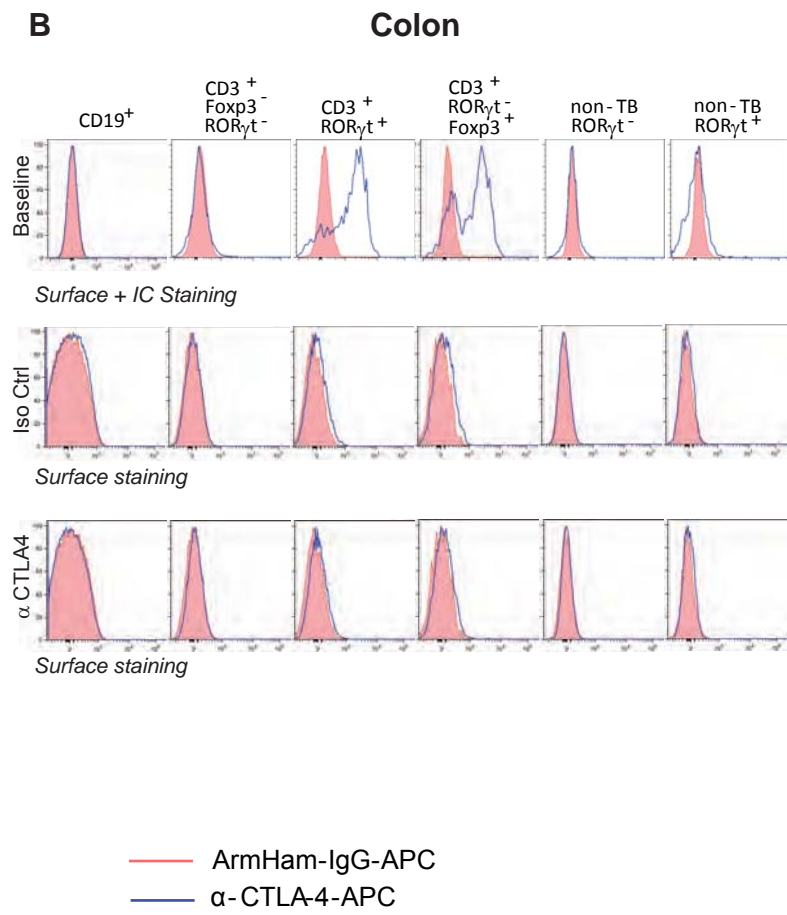
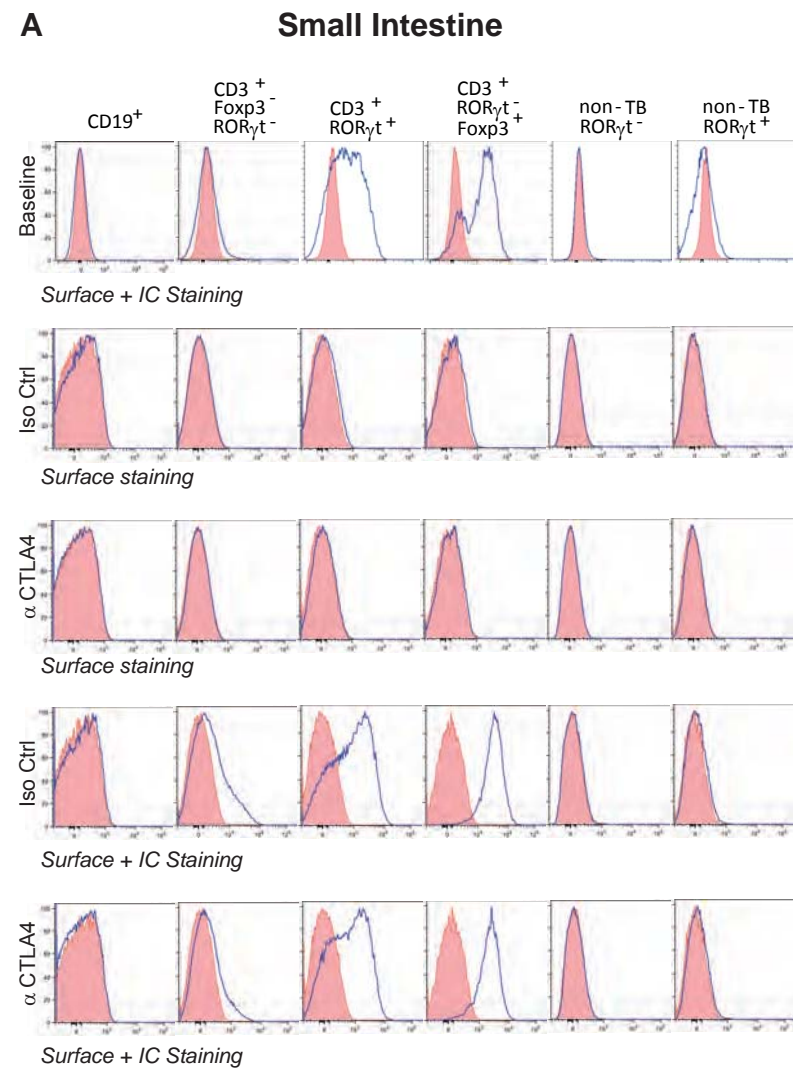
A Monosaccharide analysis by capillary electrophoresis of the capsular polysaccharide-enriched fractions from *B. fragilis* and *B. distasonis*

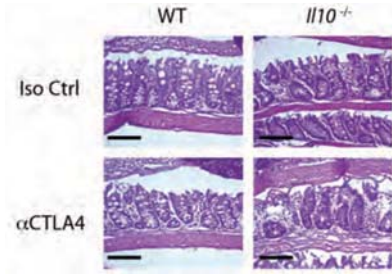
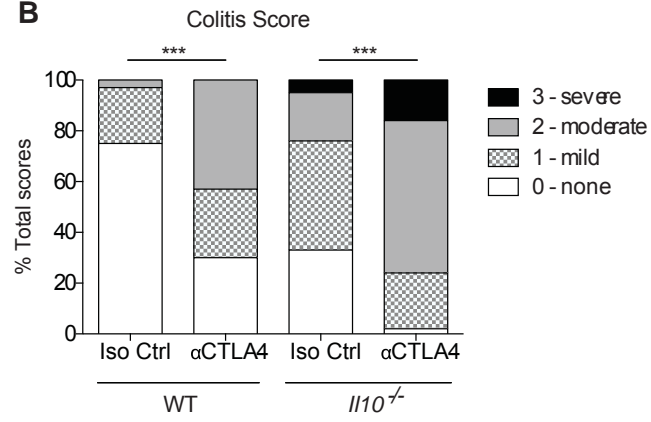
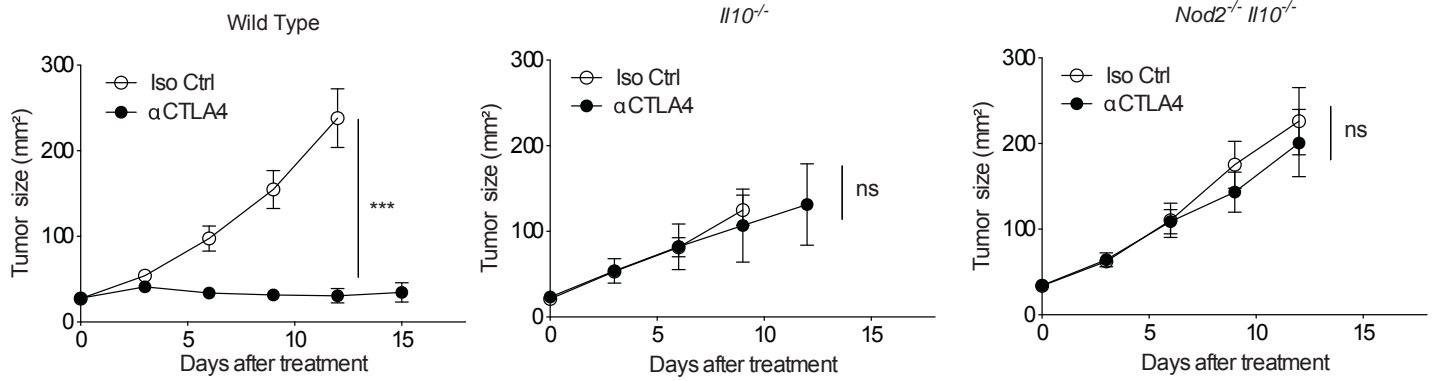


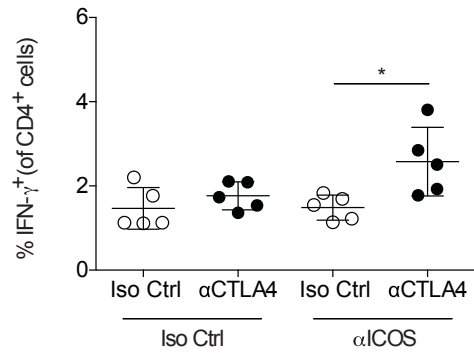
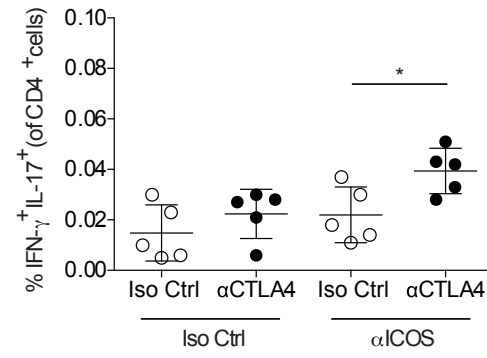
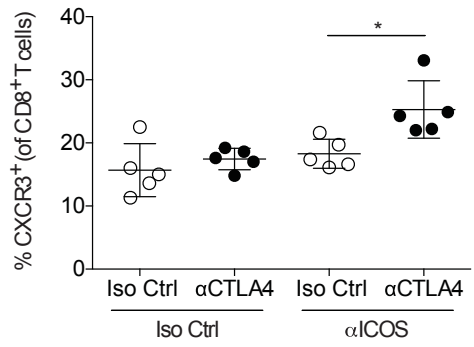
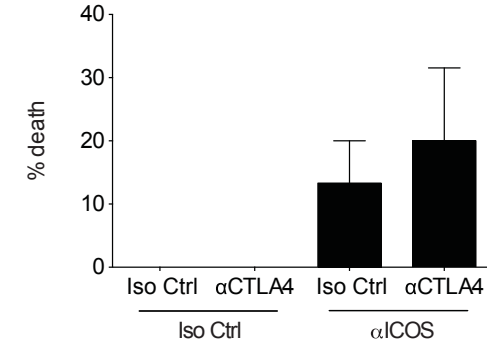
B

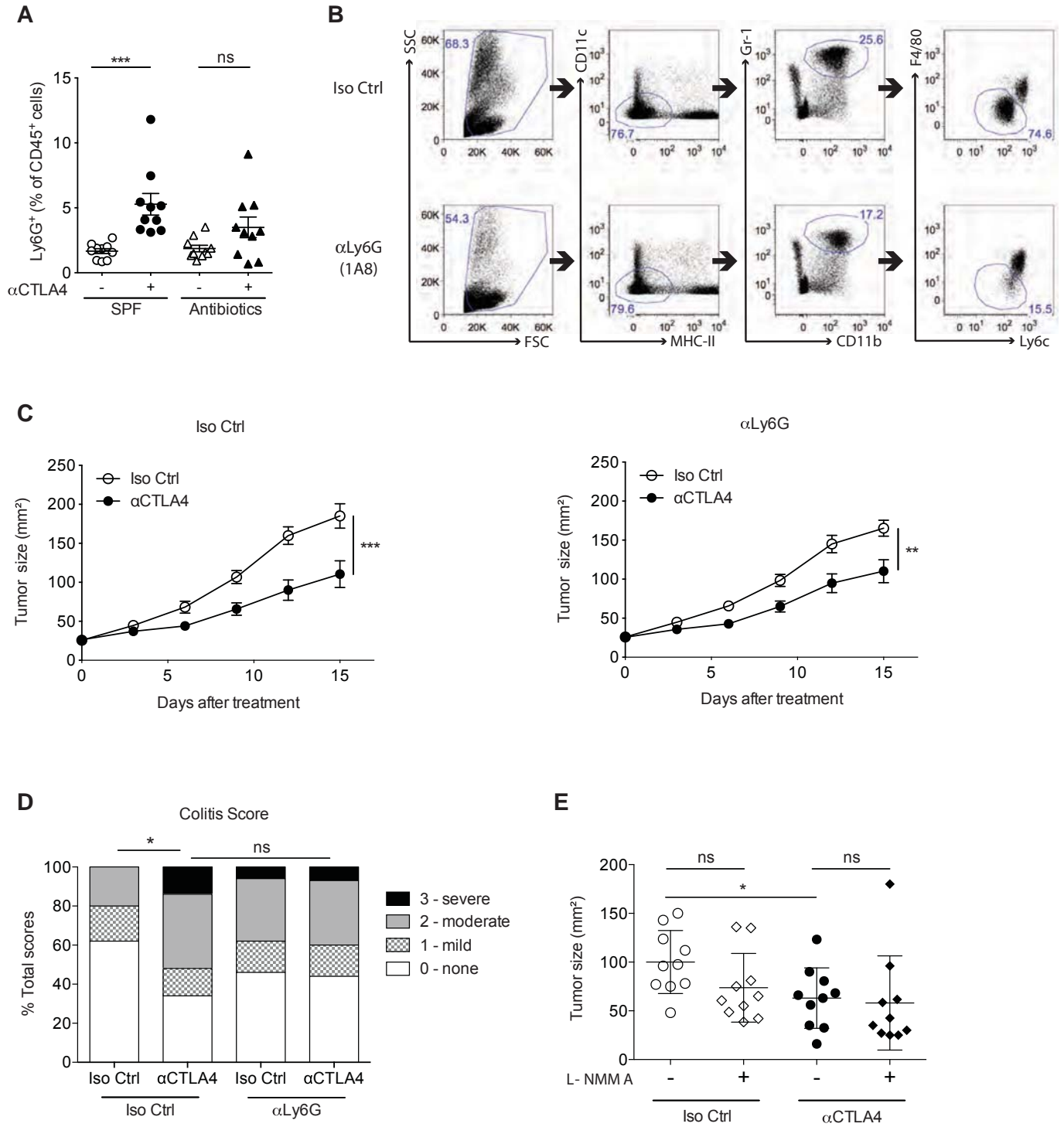




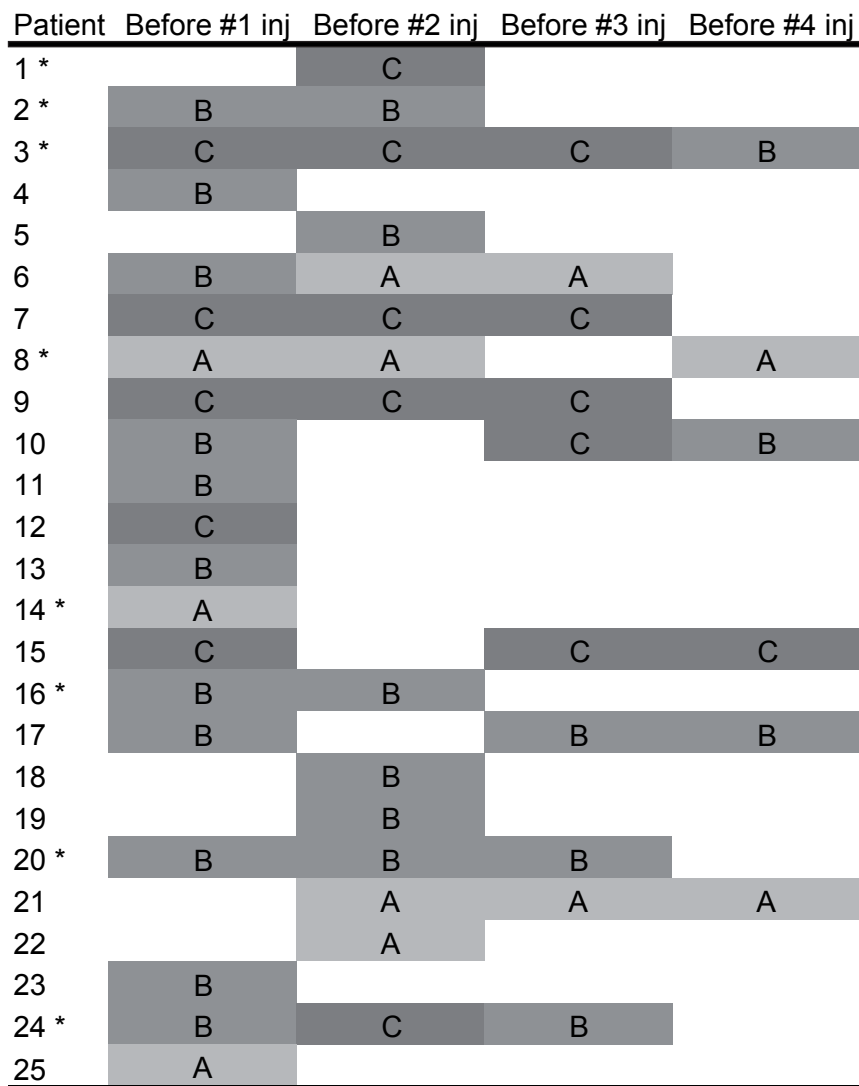


A**B****C**

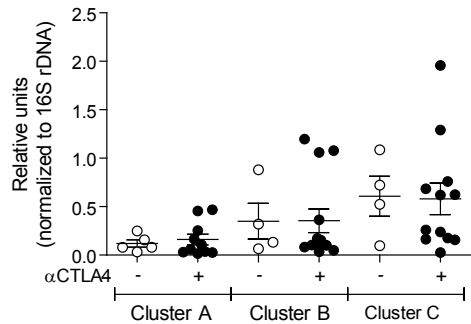
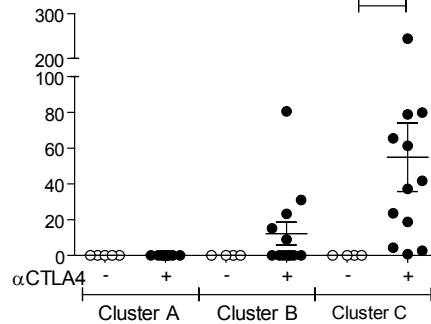
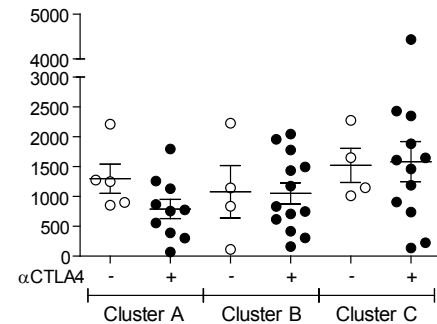
A**B****C****D**



A

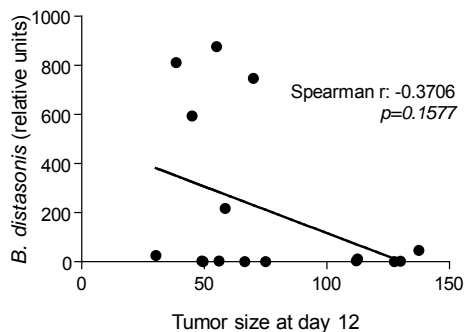


B

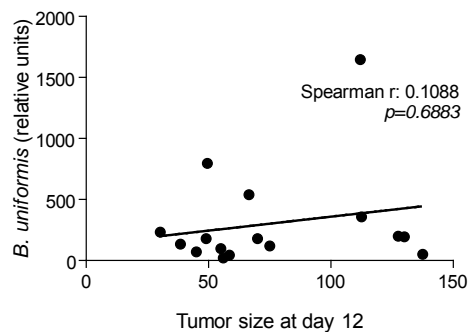
Bacteroides / Prevotella*B. fragilis**B. thetaiotaomicron*

C

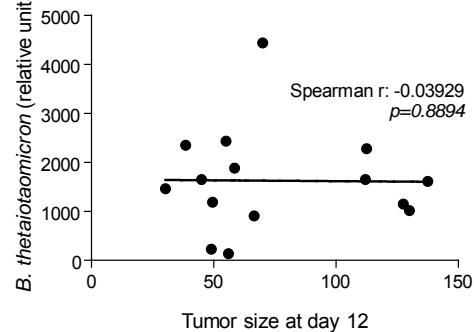
Cluster C



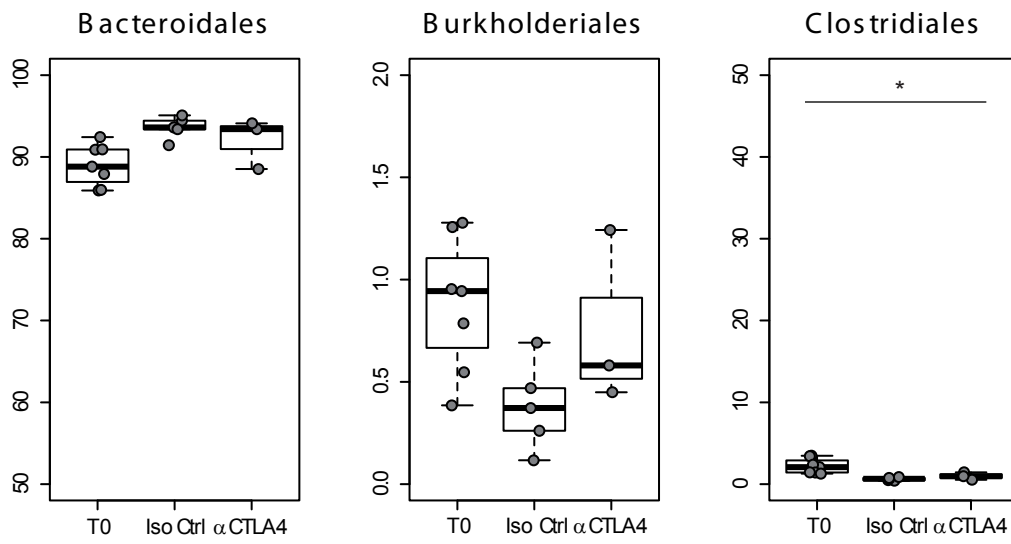
Cluster C



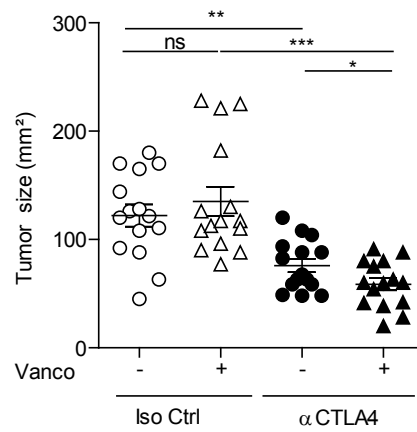
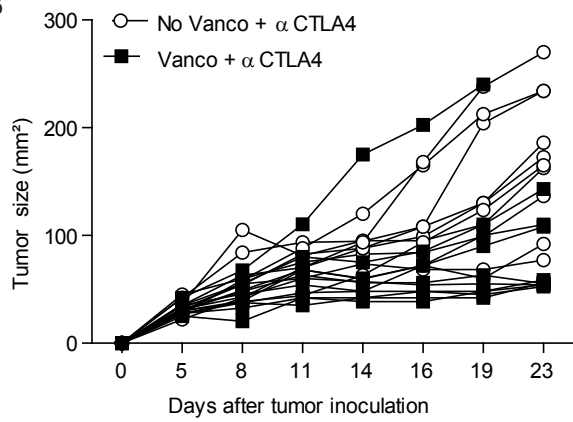
Cluster C



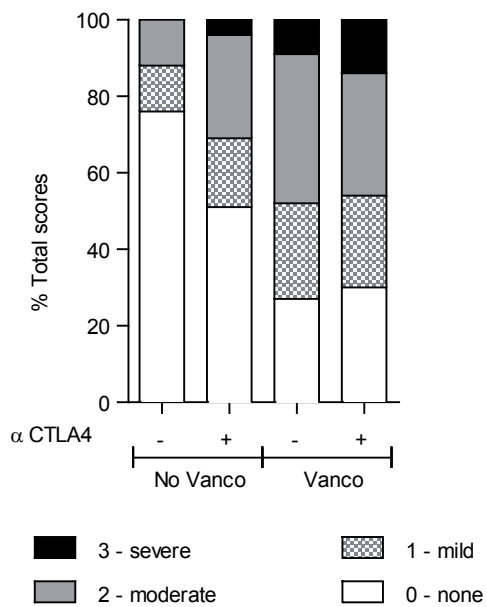
A

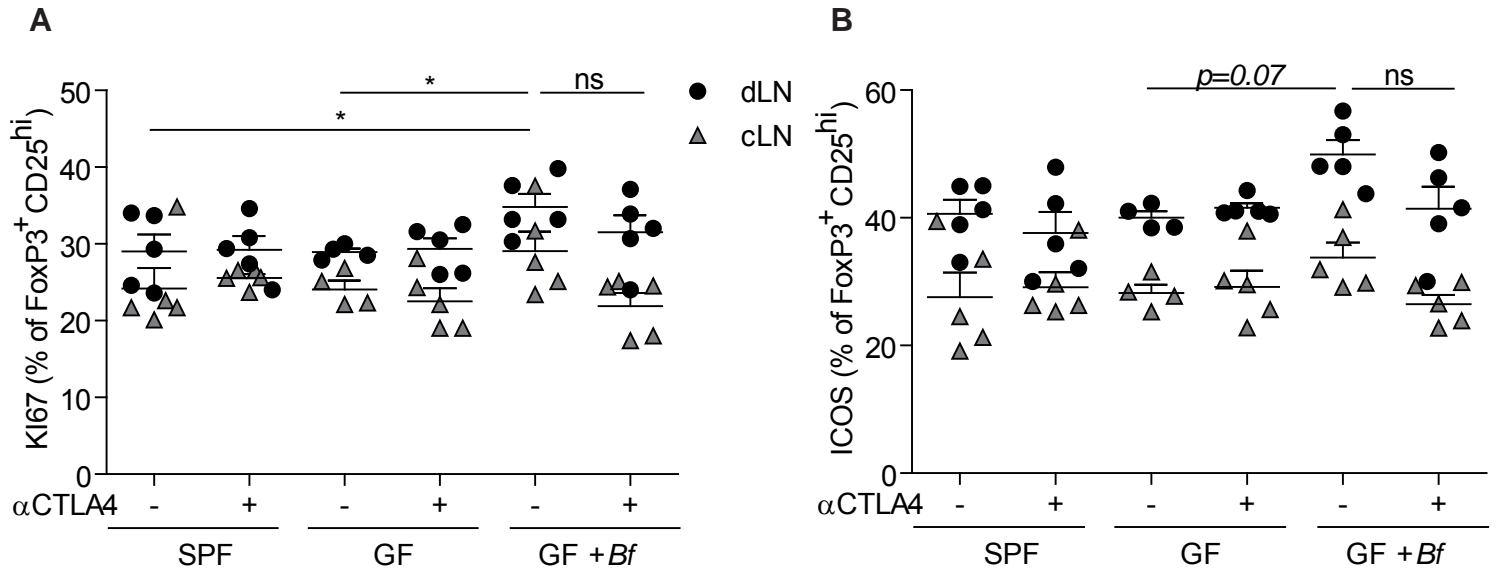


B



C





Supplemental Table 1. High throughput pyrosequencing of 16S ribosomal RNA gene amplicons of feces of naïve versus vancomycin-treated tumor bearers receiving one injection of anti-CTLA4 (9D9) Ab.

| Order | Water | | | | | | Vancomycin | | | | | |
|---|---------|-----------|--------------|----------------|------------------|--------------------|------------|-----------|--------------|----------------|------------------|--------------------|
| | Average | | | Paired T-test | | | Average | | | Paired T-test | | |
| | Water | Water_iso | Water_aCTLA4 | Ctrl vs aCTLA4 | Ctrl vs Ctrl_iso | Ctrl_iso vs aCTLA4 | Vanco | Vanco_Iso | Vanco_aCTLA4 | Ctrl vs aCTLA4 | Ctrl vs Ctrl_iso | Ctrl_iso vs aCTLA4 |
| <i>Bacteroidales</i> | 83,746 | 73,388 | 68,676 | 0,010 | 0,101 | 0,495 | 88,975 | 93,587 | 90,327 | 0,430 | 0,003 | 0,083 |
| <i>Clostridiales</i> | 9,657 | 17,416 | 24,585 | 0,012 | 0,147 | 0,299 | 2,211 | 0,630 | 1,089 | 0,029 | 0,004 | 0,048 |
| <i>Lactobacillales</i> | 1,351 | 2,993 | 2,037 | 0,482 | 0,039 | 0,413 | 3,332 | 1,379 | 2,524 | 0,386 | 0,018 | 0,140 |
| <i>Enterobacteriales</i> | 0,003 | 0,002 | 0,013 | 0,363 | 0,905 | 0,425 | 2,167 | 2,107 | 2,832 | 0,162 | 0,805 | 0,224 |
| <i>Burkholderiales</i> | 1,041 | 0,840 | 0,289 | 0,001 | 0,563 | 0,141 | 0,879 | 0,382 | 0,856 | 0,912 | 0,011 | 0,033 |
| <i>Anaeroplasmatales</i> | 0,027 | 0,005 | 0,027 | 0,995 | 0,440 | 0,326 | 1,421 | 1,212 | 1,124 | 0,167 | 0,548 | 0,784 |
| <i>Deferribacteriales</i> | 0,177 | 1,470 | 0,639 | 0,115 | 0,309 | 0,505 | 0,274 | 0,111 | 0,098 | 0,264 | 0,258 | 0,841 |
| <i>Bdellovibrionales</i> | 0,460 | 0,303 | 0,622 | 0,559 | 0,414 | 0,283 | 0,000 | 0,001 | 0,004 | 0,138 | 0,441 | 0,343 |
| <i>unclassified Firmicutes</i> | 0,182 | 0,412 | 0,706 | 0,065 | 0,160 | 0,363 | 0,000 | 0,000 | 0,004 | 0,239 | 0,356 | 0,342 |
| <i>unclassified "Bacteroidetes"</i> | 0,520 | 0,379 | 0,302 | 0,544 | 0,672 | 0,685 | 0,000 | 0,000 | 0,004 | 0,132 | nd | 0,246 |
| <i>Erysipelotrichales</i> | 0,594 | 0,307 | 0,182 | 0,090 | 0,214 | 0,154 | 0,000 | 0,000 | 0,005 | 0,116 | 0,374 | 0,240 |
| <i>Rhizobiales</i> | 0,002 | 0,000 | 0,001 | 0,500 | 0,177 | 0,286 | 0,252 | 0,076 | 0,562 | 0,062 | 0,021 | 0,036 |
| <i>Caulobacterales</i> | 0,304 | 0,075 | 0,039 | 0,084 | 0,124 | 0,330 | 0,000 | 0,000 | 0,001 | 0,039 | nd | 0,120 |
| <i>Desulfovibrionales</i> | 0,022 | 0,037 | 0,057 | 0,069 | 0,344 | 0,397 | 0,131 | 0,052 | 0,111 | 0,556 | 0,002 | 0,138 |
| <i>Selenomonadales</i> | 0,050 | 0,157 | 0,230 | 0,014 | 0,212 | 0,468 | 0,000 | 0,000 | 0,002 | 0,098 | nd | 0,205 |
| <i>Hydrogenophilales</i> | 0,155 | 0,052 | 0,004 | 0,026 | 0,111 | 0,112 | 0,000 | 0,000 | 0,001 | 0,255 | nd | 0,374 |
| <i>Verrucomicrobiales</i> | 0,010 | 0,000 | 0,003 | 0,334 | 0,153 | 0,393 | 0,011 | 0,037 | 0,065 | 0,039 | 0,210 | 0,423 |
| <i>unclassified Gammaproteobacter</i> | 0,020 | 0,016 | 0,019 | 0,912 | 0,679 | 0,798 | 0,014 | 0,001 | 0,000 | 0,424 | 0,401 | 0,307 |
| <i>unclassified Bacteria</i> | 0,014 | 0,013 | 0,030 | 0,322 | 0,868 | 0,360 | 0,000 | 0,000 | 0,000 | nd | nd | nd |
| <i>Coriobacteriales</i> | 0,018 | 0,006 | 0,012 | 0,156 | 0,004 | 0,089 | 0,000 | 0,000 | 0,001 | 0,018 | nd | 0,079 |
| <i>Bacillales</i> | 0,001 | 0,002 | 0,001 | 0,965 | 0,691 | 0,749 | 0,002 | 0,001 | 0,008 | 0,311 | 0,166 | 0,363 |
| <i>Candidatus Saccharibacteria</i> | 0,004 | 0,003 | 0,005 | 0,692 | 0,875 | 0,596 | 0,000 | 0,000 | 0,000 | nd | nd | nd |
| <i>Flavobacteriales</i> | 0,000 | 0,000 | 0,005 | 0,023 | 0,363 | 0,061 | 0,000 | 0,000 | 0,000 | nd | nd | nd |
| <i>Rhodospirillales</i> | 0,000 | 0,000 | 0,000 | nd | nd | nd | 0,001 | 0,000 | 0,002 | 0,865 | 0,032 | 0,079 |
| <i>Oceanospirillales</i> | 0,000 | 0,001 | 0,000 | 0,530 | 0,360 | 0,199 | 0,000 | 0,000 | 0,001 | 0,212 | 0,952 | 0,331 |
| <i>Pseudomonadales</i> | 0,000 | 0,001 | 0,000 | 0,297 | 0,197 | 0,313 | 0,000 | 0,000 | 0,000 | 0,851 | 0,993 | 0,856 |
| <i>Chromatiales</i> | 0,002 | 0,000 | 0,000 | 0,149 | 0,183 | 0,374 | 0,000 | 0,000 | 0,000 | nd | nd | nd |
| <i>Sphingobacteriales</i> | 0,001 | 0,000 | 0,001 | 0,645 | 0,787 | 0,489 | 0,000 | 0,000 | 0,000 | nd | nd | nd |
| <i>Rhodocyclales</i> | 0,000 | 0,000 | 0,000 | nd | nd | nd | 0,000 | 0,000 | 0,000 | 0,995 | 0,730 | 0,637 |
| <i>unclassified Alphaproteobacteria</i> | 0,001 | 0,000 | 0,000 | 0,125 | 0,235 | 0,374 | 0,000 | 0,000 | 0,000 | nd | nd | nd |
| <i>Actinomycetales</i> | 0,000 | 0,000 | 0,000 | 0,297 | nd | 0,374 | 0,000 | 0,000 | 0,001 | 0,239 | 0,356 | 0,264 |
| <i>unclassified Betaproteobacteria</i> | 0,000 | 0,000 | 0,000 | nd | nd | nd | 0,000 | 0,000 | 0,000 | 0,450 | 0,668 | 0,578 |
| <i>Cytophagales</i> | 0,000 | 0,000 | 0,000 | 0,811 | 0,999 | 0,816 | 0,000 | 0,000 | 0,000 | nd | nd | nd |
| <i>Sphingomonadales</i> | 0,000 | 0,000 | 0,000 | nd | nd | nd | 0,000 | 0,000 | 0,000 | 0,255 | 0,374 | 0,647 |

Significant differences at the level of orders of bacteria between baseline versus isotype Ctrl, and between baseline versus anti-CTLA4 Ab-treated mice and between isotype Ctrl versus anti-CTLA4 Ab-treated mice in each group of 6 mice (treated or not with vancomycin) are indicated by Student's t test. Vanco : vancomycin; Iso : Isotype Ctrl Ab

Supplemental Table 2. List of bacterial species utilized in mono-associations or in vitro assays.

| Bacteria | Strain designation | Isolation |
|---------------------------------------|---------------------------|-------------------------------------|
| <i>Bacteroides fragilis</i> | ATCC 25285 | Human, Appendix abscess |
| <i>Bacteroides thetaïotaomicron</i> | ATCC 29148 | Human, feces |
| <i>Bacteroides uniformis</i> | - | C57BL/6 mice, Mesenteric lymph node |
| <i>Burkholderia cepacia</i> | CSUR* P1210 | Human, Blood culture |
| <i>Enterococcus hirae</i> | - | C57BL/6 mice, Mesenteric lymph node |
| <i>Enterococcus faecalis</i> | JH2-2 | Ref #48 |
| <i>Escherichia coli (human study)</i> | MC1061 | Ref #49 |
| <i>Escherichia coli (mice study)</i> | - | C57BL/6 mice, Mesenteric lymph node |
| <i>Lactobacillus plantarum</i> | ATCC BAA293 | Human, Oral cavity, Saliva |
| <i>Parabacteroides disasonis</i> | - | C57BL/6 mice, feces |

CSUR* : Collection de Souches de l'Unité des Rickettsies, Marseille, France

Supplemental Table 3. Baseline characteristics of melanoma and lung cancer patients from whom PBMC were tested for memory T cells responses against bacteria

| Characteristics | No. of Patients All patients n= 27 | % |
|---|---------------------------------------|--------------------|
| Age: Mean age-yr Range -yr | 64 37-87 | |
| Sex: Male Female | 17 10 | 63 37 |
| Tumor histology: Melanoma Non-small-cell lung cancer | 11 16 | 41 59 |
| Disease stage: III IV | 2 25 | 7 93 |
| Elevated LDH* | 6 | 22 |
| Prior therapies: None Chemotherapy BRAF-inhibitor Immune check point inhibitor | 4 23 2 1 | 15 85 7 4 |
| Treatment: Ipilimumab Ipilimumab + Radiotherapy | 10 17 | 37 63 |

* LDH was not available for 14 patients

Supplemental Table 4. Characteristics of melanoma patients for whom stools were collected for high throughput sequencing analyses.

| Characteristics | No. of Patients n=25 | % |
|---|------------------------------|--------------------------------|
| Age: Mean age-yr Range -yr | 62 40-85 | |
| Sex: Male Female | 11 14 | 44 56 |
| Tumor histology: Melanoma | 25 | 100 |
| Disease stage: II III IV M1a M1b M1c | 1 6 18 2 3 13 | 4 24 72 8 12 52 |
| Elevated LDH* | 6 | 24 |
| Prior systemic therapies: None Chemotherapy Immune check point inhibitor Tyrosine kinase inhibitor | 18 3 3 1 | 72 12 12 4 |

*LDH was not available for one patient

| <i>Bacterial isolates</i> | CLUSTER A | | CLUSTER B | | CLUSTER C | | Student T-test <i>p</i> val | | |
|--|--------------|-------|--------------|-------|--------------|-------|-----------------------------|--------------------|--------------------|
| | Mean (%) | SD | Mean (%) | SD | Mean (%) | SD | Clusters A vs B | Clusters A vs C | Clusters B vs C |
| Rel. of Clostridiales bacterium 30-4c; HQ452853 | 0.001 | 0.001 | 0.004 | 0.006 | 0.001 | 0.002 | <i>0.015</i> | <i>0.668</i> | <i>0.009</i> |
| Rel. of bacterium NLAE-zl-C524; JQ608224 | 0.006 | 0.008 | 0.002 | 0.004 | 0.000 | 0.001 | <i>0.190</i> | <i>0.061</i> | <i>0.042</i> |
| Rel. of Oxalobacter formigenes; OXCR; laboratory rat cecum; U49754 | 0.004 | 0.004 | 0.002 | 0.006 | 0.001 | 0.004 | <i>0.295</i> | <i>0.065</i> | <i>0.506</i> |
| Rel. of unidentified bacterium; CCCM59; AY654959 | 0.002 | 0.006 | 0.003 | 0.010 | 0.001 | 0.002 | <i>0.664</i> | <i>0.693</i> | <i>0.353</i> |
| Rel. of Sneathiella chinensis (T); CBMAI 737; LMG 23452; DQ219355 | 0.006 | 0.013 | 0.002 | 0.005 | 0.000 | 0.001 | <i>0.432</i> | <i>0.229</i> | <i>0.128</i> |
| Rel. of Subdoligranulum variabile (T); type strain:BI 114=CCUG 47106=DSM 15176; AJ518869 | 0.003 | 0.004 | 0.002 | 0.003 | 0.002 | 0.002 | <i>0.342</i> | <i>0.218</i> | <i>0.648</i> |
| Rel. of Clostridiaceae bacterium DJF_LS13; EU728741 | 0.004 | 0.010 | 0.002 | 0.003 | 0.001 | 0.002 | <i>0.445</i> | <i>0.253</i> | <i>0.130</i> |
| Rel. of bacterium MB7-1; DQ453797 | 0.000 | 0.000 | 0.005 | 0.017 | 0.000 | 0.000 | <i>0.214</i> | <i>na</i> | <i>0.214</i> |
| Rel. of Ruminococcus flavefaciens; AR72; AF104841 | 0.004 | 0.009 | 0.002 | 0.006 | 0.000 | 0.001 | <i>0.641</i> | <i>0.232</i> | <i>0.098</i> |
| Rel. of bacterium NLAE-zl-C265; JQ607983 | 0.005 | 0.013 | 0.002 | 0.003 | 0.000 | 0.001 | <i>0.503</i> | <i>0.307</i> | <i>0.040</i> |
| Rel. of Gram-negative bacterium cTPY-13; AY239461 | 0.005 | 0.016 | 0.001 | 0.002 | 0.002 | 0.005 | <i>0.389</i> | <i>0.491</i> | <i>0.566</i> |
| Rel. of Enterobacter sp. SWF66517; GU122156 | 0.001 | 0.002 | 0.004 | 0.007 | 0.000 | 0.001 | <i>0.035</i> | <i>0.506</i> | <i>0.018</i> |
| Rel. of Clostridiaceae bacterium NML 060002; EU815225 | 0.000 | 0.001 | 0.004 | 0.006 | 0.001 | 0.002 | <i>0.028</i> | <i>0.557</i> | <i>0.069</i> |
| Rel. of Lactobacillus paraplantarum (T); DSM 10667T; AJ306297 | 0.000 | 0.000 | 0.004 | 0.016 | 0.000 | 0.001 | <i>0.205</i> | <i>0.169</i> | <i>0.225</i> |
| Rel. of bacterium str. 31285; AF227834 | 0.000 | 0.001 | 0.004 | 0.006 | 0.001 | 0.002 | <i>0.021</i> | <i>0.780</i> | <i>0.030</i> |
| Rel. of Clostridium sp. cTPY-17; AY239462 | 0.002 | 0.002 | 0.003 | 0.014 | 0.000 | 0.000 | <i>0.633</i> | <i>0.035</i> | <i>0.276</i> |

REFERENCES

1. K. S. Peggs, S. A. Quezada, A. J. Korman, J. P. Allison, Principles and use of anti-CTLA4 antibody in human cancer immunotherapy. *Curr. Opin. Immunol.* **18**, 206–213 (2006). [Medline doi:10.1016/j.coi.2006.01.011](#)
2. F. S. Hodi, S. J. O'Day, D. F. McDermott, R. W. Weber, J. A. Sosman, J. B. Haanen, R. Gonzalez, C. Robert, D. Schadendorf, J. C. Hassel, W. Akerley, A. J. van den Eertwegh, J. Lutzky, P. Lorigan, J. M. Vaubel, G. P. Linette, D. Hogg, C. H. Ottensmeier, C. Lebbé, C. Peschel, I. Quirt, J. I. Clark, J. D. Wolchok, J. S. Weber, J. Tian, M. J. Yellin, G. M. Nichol, A. Hoos, W. J. Urba, Improved survival with ipilimumab in patients with metastatic melanoma. *N. Engl. J. Med.* **363**, 711–723 (2010). [Medline doi:10.1056/NEJMoal003466](#)
3. K. E. Beck, J. A. Blansfield, K. Q. Tran, A. L. Feldman, M. S. Hughes, R. E. Royal, U. S. Kammula, S. L. Topalian, R. M. Sherry, D. Kleiner, M. Quezado, I. Lowy, M. Yellin, S. A. Rosenberg, J. C. Yang, Enterocolitis in patients with cancer after antibody blockade of cytotoxic T-lymphocyte-associated antigen 4. *J. Clin. Oncol.* **24**, 2283–2289 (2006). [Medline doi:10.1200/JCO.2005.04.5716](#)
4. D. Berman, S. M. Parker, J. Siegel, S. D. Chasalow, J. Weber, S. Galbraith, S. R. Targan, H. L. Wang, Blockade of cytotoxic T-lymphocyte antigen-4 by ipilimumab results in dysregulation of gastrointestinal immunity in patients with advanced melanoma. *Cancer Immun.* **10**, 11 (2010). [Medline](#)
5. S. Viaud, F. Saccheri, G. Mignot, T. Yamazaki, R. Daillère, D. Hannani, D. P. Enot, C. Pfirschke, C. Engblom, M. J. Pittet, A. Schlitzer, F. Ginhoux, L. Apetoh, E. Chachaty, P. L. Woerther, G. Eberl, M. Bérard, C. Ecobichon, D. Clermont, C. Bizet, V. Gaboriau-Routhiau, N. Cerf-Bensussan, P. Opolon, N. Yessaad, E. Vivier, B. Ryffel, C. O. Elson, J. Doré, G. Kroemer, P. Lepage, I. G. Boneca, F. Ghiringhelli, L. Zitvogel, The intestinal microbiota modulates the anticancer immune effects of cyclophosphamide. *Science* **342**, 971–976 (2013). [Medline doi:10.1126/science.1240537](#)
6. A. Rogoz, B. S. Reis, R. A. Karssemeijer, D. Mucida, A 3-D enteroid-based model to study T-cell and epithelial cell interaction. *J. Immunol. Methods* **421**, 89–95 (2015). [Medline doi:10.1016/j.jim.2015.03.014](#)
7. S. Dasgupta, D. Erturk-Hasdemir, J. Ochoa-Reparaz, H. C. Reinecker, D. L. Kasper, Plasmacytoid dendritic cells mediate anti-inflammatory responses to a gut commensal molecule via both innate and adaptive mechanisms. *Cell Host Microbe* **15**, 413–423 (2014). [Medline](#)
8. S. K. Mazmanian, C. H. Liu, A. O. Tzianabos, D. L. Kasper, An immunomodulatory molecule of symbiotic bacteria directs maturation of the host immune system. *Cell* **122**, 107–118 (2005). [Medline doi:10.1016/j.cell.2005.05.007](#)
9. F. Stinglele, B. Corthésy, N. Kusy, S. A. Porcelli, D. L. Kasper, A. O. Tzianabos, Zwitterionic polysaccharides stimulate T cells with no preferential V beta usage and promote anergy, resulting in protection against experimental abscess formation. *J. Immunol.* **172**, 1483–1490 (2004). [Medline doi:10.4049/jimmunol.172.3.1483](#)

10. A. O. Tzianabos, A. Pantosti, H. Baumann, J. R. Brisson, H. J. Jennings, D. L. Kasper, The capsular polysaccharide of *Bacteroides fragilis* comprises two ionically linked polysaccharides. *J. Biol. Chem.* **267**, 18230–18235 (1992). [Medline](#)
11. J. Y. Huang, S. M. Lee, S. K. Mazmanian, The human commensal *Bacteroides fragilis* binds intestinal mucin. *Anaerobe* **17**, 137–141 (2011). [Medline](#)
[doi:10.1016/j.anaerobe.2011.05.017](https://doi.org/10.1016/j.anaerobe.2011.05.017)
12. M. Arumugam, J. Raes, E. Pelletier, D. Le Paslier, T. Yamada, D. R. Mende, G. R. Fernandes, J. Tap, T. Bruls, J. M. Batto, M. Bertalan, N. Borrueel, F. Casellas, L. Fernandez, L. Gautier, T. Hansen, M. Hattori, T. Hayashi, M. Kleerebezem, K. Kurokawa, M. Leclerc, F. Levenez, C. Manichanh, H. B. Nielsen, T. Nielsen, N. Pons, J. Poulain, J. Qin, T. Sicheritz-Ponten, S. Tims, D. Torrents, E. Ugarte, E. G. Zoetendal, J. Wang, F. Guarner, O. Pedersen, W. M. de Vos, S. Brunak, J. Doré, M. Antolín, F. Artiguenave, H. M. Blottiere, M. Almeida, C. Brechot, C. Cara, C. Chervaux, A. Cultrone, C. Delorme, G. Denariáz, R. Dervyn, K. U. Foerstner, C. Friss, M. van de Guchte, E. Guedon, F. Haimet, W. Huber, J. van Hylckama-Vlieg, A. Jamet, C. Juste, G. Kaci, J. Knol, O. Lakhdari, S. Layec, K. Le Roux, E. Maguin, A. Mérieux, R. Melo Minardi, C. M'rini, J. Muller, R. Oozeer, J. Parkhill, P. Renault, M. Rescigno, N. Sanchez, S. Sunagawa, A. Torrejon, K. Turner, G. Vandemeulebrouck, E. Varela, Y. Winogradsky, G. Zeller, J. Weissenbach, S. D. Ehrlich, P. Bork; MetaHIT Consortium, Enterotypes of the human gut microbiome. *Nature* **473**, 174–180 (2011). [Medline](#)
[doi:10.1038/nature09944](https://doi.org/10.1038/nature09944)
13. J. Qin, R. Li, J. Raes, M. Arumugam, K. S. Burgdorf, C. Manichanh, T. Nielsen, N. Pons, F. Levenez, T. Yamada, D. R. Mende, J. Li, J. Xu, S. Li, D. Li, J. Cao, B. Wang, H. Liang, H. Zheng, Y. Xie, J. Tap, P. Lepage, M. Bertalan, J.-M. Batto, T. Hansen, D. Le Paslier, A. Linneberg, H. B. Nielsen, E. Pelletier, P. Renault, T. Sicheritz-Ponten, K. Turner, H. Zhu, C. Yu, S. Li, M. Jian, Y. Zhou, Y. Li, X. Zhang, S. Li, N. Qin, H. Yang, J. Wang, S. Brunak, J. Doré, F. Guarner, K. Kristiansen, O. Pedersen, J. Parkhill, J. Weissenbach, P. Bork, S. D. Ehrlich, J. Wang; MetaHIT Consortium, A human gut microbial gene catalogue established by metagenomic sequencing. *Nature* **464**, 59–65 (2010). [Medline](#)
[doi:10.1038/nature08821](https://doi.org/10.1038/nature08821)
14. A. Cebula, M. Seweryn, G. A. Rempala, S. S. Pabla, R. A. McIndoe, T. L. Denning, L. Bry, P. Kraj, P. Kisielow, L. Ignatowicz, Thymus-derived regulatory T cells contribute to tolerance to commensal microbiota. *Nature* **497**, 258–262 (2013). [Medline](#)
[doi:10.1038/nature12079](https://doi.org/10.1038/nature12079)
15. J. L. Sonnenburg, C. T. Chen, J. I. Gordon, Genomic and metabolic studies of the impact of probiotics on a model gut symbiont and host. *PLOS Biol.* **4**, e413 (2006). [Medline](#)
[doi:10.1371/journal.pbio.0040413](https://doi.org/10.1371/journal.pbio.0040413)
16. W. Lam, S. Bussom, F. Guan, Z. Jiang, W. Zhang, E. A. Gullen, S. H. Liu, Y. C. Cheng, The four-herb Chinese medicine PHY906 reduces chemotherapy-induced gastrointestinal toxicity. *Sci. Transl. Med.* **2**, 45ra59 (2010). [Medline](#) [doi:10.1126/scitranslmed.3001270](https://doi.org/10.1126/scitranslmed.3001270)
17. H. Xu, J. Yang, W. Gao, L. Li, P. Li, L. Zhang, Y. N. Gong, X. Peng, J. J. Xi, S. Chen, F. Wang, F. Shao, Innate immune sensing of bacterial modifications of Rho GTPases by the P2Y₁₂ inflammasome. *Nature* **513**, 237–241 (2014). [Medline](#) [doi:10.1038/nature13449](https://doi.org/10.1038/nature13449)

18. M. Mimee, A. C. Tucker, C. A. Voigt, T. K. Lu, Programming a human commensal bacterium, *Bacteroides thetaiotaomicron*, to sense and respond to stimuli in the murine gut microbiota. *Cell Systems* **1**, 62–71 (2015). [doi:10.1016/j.cels.2015.06.001](https://doi.org/10.1016/j.cels.2015.06.001)
19. M. Venkatesh, S. Mukherjee, H. Wang, H. Li, K. Sun, A. P. Benechet, Z. Qiu, L. Maher, M. R. Redinbo, R. S. Phillips, J. C. Fleet, S. Kortagere, P. Mukherjee, A. Fasano, J. Le Ven, J. K. Nicholson, M. E. Dumas, K. M. Khanna, S. Mani, Symbiotic bacterial metabolites regulate gastrointestinal barrier function via the xenobiotic sensor PXR and Toll-like receptor 4. *Immunity* **41**, 296–310 (2014). [Medline](https://pubmed.ncbi.nlm.nih.gov/24781111/) [doi:10.1016/j.immuni.2014.06.014](https://doi.org/10.1016/j.immuni.2014.06.014)
20. C. A. Schneider, W. S. Rasband, K. W. Eliceiri, NIH Image to ImageJ: 25 years of image analysis. *Nat. Methods* **9**, 671–675 (2012). [Medline](https://pubmed.ncbi.nlm.nih.gov/22755421/) [doi:10.1038/nmeth.2089](https://doi.org/10.1038/nmeth.2089)
21. R. I. Amann, B. J. Binder, R. J. Olson, S. W. Chisholm, R. Devereux, D. A. Stahl, Combination of 16S rRNA-targeted oligonucleotide probes with flow cytometry for analyzing mixed microbial populations. *Appl. Environ. Microbiol.* **56**, 1919–1925 (1990). [Medline](https://pubmed.ncbi.nlm.nih.gov/1951111/)
22. A. H. Franks, H. J. Harmsen, G. C. Raangs, G. J. Jansen, F. Schut, G. W. Welling, Variations of bacterial populations in human feces measured by fluorescent in situ hybridization with group-specific 16S rRNA-targeted oligonucleotide probes. *Appl. Environ. Microbiol.* **64**, 3336–3345 (1998). [Medline](https://pubmed.ncbi.nlm.nih.gov/9711111/)
23. L. Rigottier-Gois, V. Rochet, N. Garrec, A. Suau, J. Doré, Enumeration of *Bacteroides* species in human faeces by fluorescent in situ hybridisation combined with flow cytometry using 16S rRNA probes. *Syst. Appl. Microbiol.* **26**, 110–118 (2003). [Medline](https://pubmed.ncbi.nlm.nih.gov/12711111/) [doi:10.1078/072320203322337399](https://doi.org/10.1078/072320203322337399)
24. A. Schlitzer, N. McGovern, P. Teo, T. Zelante, K. Atarashi, D. Low, A. W. Ho, P. See, A. Shin, P. S. Wasan, G. Hoeffel, B. Malleret, A. Heiseke, S. Chew, L. Jardine, H. A. Purvis, C. M. Hilken, J. Tam, M. Poidinger, E. R. Stanley, A. B. Krug, L. Renia, B. Sivasankar, L. G. Ng, M. Collin, P. Ricciardi-Castagnoli, K. Honda, M. Haniffa, F. Ginhoux, IRF4 transcription factor-dependent CD11b⁺ dendritic cells in human and mouse control mucosal IL-17 cytokine responses. *Immunity* **38**, 970–983 (2013). [Medline](https://pubmed.ncbi.nlm.nih.gov/24111111/) [doi:10.1016/j.immuni.2013.04.011](https://doi.org/10.1016/j.immuni.2013.04.011)
25. A. Pantosti, A. O. Tzianabos, A. B. Onderdonk, D. L. Kasper, Immunochemical characterization of two surface polysaccharides of *Bacteroides fragilis*. *Infect. Immun.* **59**, 2075–2082 (1991). [Medline](https://pubmed.ncbi.nlm.nih.gov/13111111/)
26. F. T. Chen, T. S. Dobashi, R. A. Evangelista, Quantitative analysis of sugar constituents of glycoproteins by capillary electrophoresis. *Glycobiology* **8**, 1045–1052 (1998). [Medline](https://pubmed.ncbi.nlm.nih.gov/9811111/) [doi:10.1093/glycob/8.11.1045](https://doi.org/10.1093/glycob/8.11.1045)
27. J. Nigou, A. Vercellone, G. Puzo, New structural insights into the molecular deciphering of mycobacterial lipoglycan binding to C-type lectins: Lipoarabinomannan glycoform characterization and quantification by capillary electrophoresis at the subnanomole level. *J. Mol. Biol.* **299**, 1353–1362 (2000). [Medline](https://pubmed.ncbi.nlm.nih.gov/11111111/) [doi:10.1006/jmbi.2000.3821](https://doi.org/10.1006/jmbi.2000.3821)
28. H. Baumann, A. O. Tzianabos, J. R. Brisson, D. L. Kasper, H. J. Jennings, Structural elucidation of two capsular polysaccharides from one strain of *Bacteroides fragilis* using

- high-resolution NMR spectroscopy. *Biochemistry* **31**, 4081–4089 (1992). [Medline doi:10.1021/bi00131a026](#)
29. T. Sato, R. G. Vries, H. J. Snippert, M. van de Wetering, N. Barker, D. E. Stange, J. H. van Es, A. Abo, P. Kujala, P. J. Peters, H. Clevers, Single Lgr5 stem cells build crypt-villus structures in vitro without a mesenchymal niche. *Nature* **459**, 262–265 (2009). [Medline doi:10.1038/nature07935](#)
 30. J.-P. Furet, O. Firmesse, M. Gourmelon, C. Bridonneau, J. Tap, S. Mondot, J. Doré, G. Corthier, Comparative assessment of human and farm animal faecal microbiota using real-time quantitative PCR. *FEMS Microbiol. Ecol.* **68**, 351–362 (2009). [Medline doi:10.1111/j.1574-6941.2009.00671.x](#)
 31. M. T. Suzuki, L. T. Taylor, E. F. DeLong, Quantitative analysis of small-subunit rRNA genes in mixed microbial populations via 5'-nuclease assays. *Appl. Environ. Microbiol.* **66**, 4605–4614 (2000). [Medline doi:10.1128/AEM.66.11.4605-4614.2000](#)
 32. W. Manz, R. Amann, W. Ludwig, M. Vancanneyt, K.-H. Schleifer, Application of a suite of 16S rRNA-specific oligonucleotide probes designed to investigate bacteria of the phylum cytophaga-flavobacter-bacteroides in the natural environment. *Microbiology* **142**, 1097–1106 (1996). [Medline doi:10.1099/13500872-142-5-1097](#)
 33. T. Odamaki, J. Z. Xiao, M. Sakamoto, S. Kondo, T. Yaeshima, K. Iwatsuki, H. Togashi, T. Enomoto, Y. Benno, Distribution of different species of the *Bacteroides fragilis* group in individuals with Japanese cedar pollinosis. *Appl. Environ. Microbiol.* **74**, 6814–6817 (2008). [Medline doi:10.1128/AEM.01106-08](#)
 34. S. M. Lee, G. P. Donaldson, Z. Mikulski, S. Boyajian, K. Ley, S. K. Mazmanian, Bacterial colonization factors control specificity and stability of the gut microbiota. *Nature* **501**, 426–429 (2013). [Medline doi:10.1038/nature12447](#)
 35. J. Tong, C. Liu, P. Summanen, H. Xu, S. M. Finegold, Application of quantitative real-time PCR for rapid identification of *Bacteroides fragilis* group and related organisms in human wound samples. *Anaerobe* **17**, 64–68 (2011). [Medline doi:10.1016/j.anaerobe.2011.03.004](#)